NASA Technical Memorandum

NASA TM-86473

RESULTS OF THE TECHNICAL EXCHANGE AGREEMENT BETWEEN NASA AND DuPONT ON THE CONTAINERLESS DROP TUBE SOLIDIFICATION OF $NiAl_3$

By Edwin C. Ethridge, Peter A. Curreri, and Michael Kelly

Space Science Laboratory

October 1984

National Aeronautics and Space Administration

George C. Marshall Space Flight Center

TECHNICAL REPORT STANDARD TITLE PAGE

1. REPORT NO.	2. GOVERNMENT ACCESSION NO.	3. RECIPIENT'S CATALOG NO.
NASA TM-86473		

4. TITLE AND SUBTITLE	5. REPORT DATE
Results of the Technical Exchange Agreement Between NASA and DuPont on the Containerless Drop Tube Solidification of $NiAl_3$	October 1984
	6. PERFORMING ORGANIZATION CODE
7. AUTHOR(S)	8. PERFORMING ORGANIZATION REPORT #
Edwin C. Ethridge, Peter A. Curreri, and Michael Kelly*	
9. PERFORMING ORGANIZATION NAME AND ADDRESS	10. WORK UNIT NO.
George C. Marshall Space Flight Center Marshall Space Flight Center, Alabama 35812	11. CONTRACT OR GRANT NO.
	13. TYPE OF REPORT & PERIOD COVERED
12. SPONSORING AGENCY NAME AND ADDRESS	Technical Memorandum
National Aeronautics and Space Administration Washington, D.C. 20546	14. SPONSORING AGENCY CODE

15. SUPPLEMENTARY NOTES

Prepared by Space Science Laboratory, Science and Engineering Directorate.
*E. I. Du Pont de Nemours Company, Wilmington, Delaware.

16. ABSTRACT

The final results of the Drop Tube Solidification of $NiAl_3$ are presented. Problems associated with the utilization of a "dripper" furnace in the drop tube are discussed and the modification of experimental procedures required to achieve results are described. Sample microstructures of drop tube samples are compared with other samples. The dendrite arm spacings of drop tube samples are correlated with the rapid cooling rates.

17. KEY WORDS	18. DISTRIBUTION STATEMENT
Drop Tube Containerless Solidification $NiAl_3$ Dendrite Arm Spacings	Unclassified – Unlimited E. C. Ethridge

19. SECURITY CLASSIF. (of this report)	20. SECURITY CLASSIF. (of this page)	21. NO. OF PAGES	22. PRICE
Unclassified	Unclassified	45	NTIS

MSFC - Form 3292 (May 1969)

For sale by National Technical Information Service, Springfield, Virginia 22151

ACKNOWLEDGMENTS

Appreciation is expressed to Alice Dorries for taking the SEM EDXA data and to Dr. Gary Workman, Robert Bond, and Anita Mobely-Smith for performing some of the drop tube experiments. We would also like to acknowledge Jerry Johnson and Bill Aldrich for developing the furnaces used in the study. This work was supported in part by R. E. Halpern in the Microgravity Science Division of NASA Headquarters.

TABLE OF CONTENTS

LIST OF ILLUSTRATIONS

LIST OF ILLUSTRATIONS (Concluded)

TECHNICAL MEMORANDUM

RESULTS OF THE TECHNICAL EXCHANGE AGREEMENT BETWEEN NASA AND DuPONT ON THE CONTAINERLESS DROP TUBE SOLIDIFICATION OF $NiAl_3$

INTRODUCTION

The purpose of this report is to describe the results obtained by experiments on the drop tube solidification of $NiAl_3$. This work results from a new approach by NASA for introducing industry to the materials processing in space program [1]. In January 1982 a technical exchange agreement between NASA and E. I. DuPont de Nemours was signed, officially initiating the research.

Ni-Al alloys rich in Al are Raney catalyst materials. In general Raney alloys consist of two metallic components. One is the dispersed catalytically-active transition metal component and can be any one of a number of the non-noble or noble transition metals (Rh, Ni, Pt, etc.). A matrix component such as Al, Si, Zn, or Mg constitutes the second phase. The matrix component is selected such that it is susceptible to chemical dissolution by either acid or alkaline leaching. With the $NiAl_3$ catalysts, upon reacting with caustic aqueous solution, the Al atoms preferentially leach out of the alloy leaving behind an ultrahigh, surface-area-active Ni sponge. This sponge is catalytically active and is used for a number of chemical reactions such as the methanation of hydrogen and carbon monoxide to methane and water [2], the steam re-formation of hydrocarbons, and hydrogenation reactions [3-6].

The objective of the work was to containerlessly solidify samples of an Ni-Al alloy with a composition close to that of the compound $NiAl_3$. It has been demonstrated that the $NiAl_3$ eta phase is catalytically the most active component of a Raney-type alloy [2,7] such that the overall activity of Raney Ni depends mainly on the $NiAl_3$ phase content of the alloy [3]. The desired result was the formation of a high percentage of the $NiAl_3$ compound with minimal amounts of the other surrounding compounds Ni_2Al_3 (delta phase) and Al solid solution.

The present study was undertaken in order to investigate the possibility of undercooling Al-Ni alloys well below the liquidus in order to produce a single phase peritectic structure by containerless drop tube solidification. Containerless processing is a technique for both high purity contamination free studies, as well as for investigating the undercooling of alloys.

In order to achieve large undercoolings one must avoid nucleation of crystallization. Nucleation can proceed by one of two processes. Homogeneous nucleation is that nucleation of crystal phases that occurs due to the statistical fluctuation of nuclei until nuclei of a critical size are formed that are stable and grow. Heterogeneous nucleation, on the other hand, results from the catalysis of crystal growth by the presence of solid surfaces that lower the surface free energy term permitting a smaller critical nucleus radius to be stable. In normal processing techniques, the melt solidifies in contact with a crucible or container and is susceptible to

heterogeneous nucleation. Presumably with containerless solidification in a drop tube, the crucible is eliminated and heterogeneous nucleation is minimized, permitting larger undercoolings than are possible with traditional techniques.

Initial estimates of homogeneous nucleation rates by Turnbull and Cech [8] indicated that at undercoolings of about 0.2 of the absolute melting temperature, Tm, homogeneous nucleation would predominate limiting further undercooling. More recent investigations of fine dispersions of low melting alloys have shown that undercoolings of 0.3 Tm are common and some metals such as Ga may be undercooled to about 0.5 Tm prior to spontaneous nucleation [9].

Containerless melting and solidification of metals in free fall have been shown to be an effective means of achieving large undercoolings and unique microstructures. Lacy et al. [10] and Robinson [11] achieved undercoolings of 500° and 525°C for Nb-Ge and Nb, respectively. Utilizing containerless solidification during free fall down a drop tube, a superconducting metastable peritectic phase in the Nb-Ge system has been formed. In other studies, molten droplets of Pd-Si-Cu were containerlessly solidified in free fall down the drop tube to form bulk amorphous spheres [12].

The Marshall Space Flight Center drop tubes are unique facilities for containerless processing experiments. It was intended that the molten droplets that were formed would experience containerless solidification as they fell down the drop tube. It was hoped that when they solidified, the temperature would be below the peritectic temperature and the samples would solidify predominantly to the desired peritectic phase $NiAl_3$. Based on these results it seemed that the undercoolings of $NiAl_3$ as molten droplets in free fall down the MSFC drop tube might be possible.

EXPERIMENTAL PROCEDURE

The desired result in these experiments was to produce molten droplets about 0.5 and 2 mm in diameter that would freely drop from the crucible and fall down the drop tube. A laboratory vacuum system and bell jar were used to test the melting and droplet formation process. For these experiments molten samples were dropped into diffusion vacuum pump oil after falling about 3 ft. These experiments were used to test the dripper assembly and for comparison with the containerless solidified samples. When successful drops were verified in the laboratory, the furnace was transferred to the 100-ft drop tube at the Marshall Space Flight Center to process a number of samples in free fall (Fig. 1). This facility consists of a 6-in.-diameter stainless steel vertical tube about 100 ft long with a bell jar assembly connected to the top (Fig. 2) and a removable sample catcher at the bottom (Fig. 3). Two pumping stations, each consisting of a mechanical roughing pump and a turbomolecular vacuum pump, are located at the top and bottom. The drop tube is instrumented with vacuum gauges and temperature measuring sensors through a Hewlett Packard 9835 microcomputer.

Two types of furnaces were used to melt the samples inside the drop tube bell jar. The first is a transparent furnace [Johnson, 1982, NASA/MSFC, personal communication]. It has a simple design, consisting of a refractory metal heating coil wound around a tube of fused silica (quartz) or alumina (Figs. 4 and 5). Two types of heating element wire were used in the furnace, Pt and W-26Re. The crucible was situated inside the tube, and the coil was wound around the outside. The fused silica tubes were provided with small mounds of fused silica attached to the outside

of the quartz tube to keep the heating element coils separated (Fig. 6). For other tests, the heating coil was placed on an alumina tube, and a high purity alumina refractory cement was used to coat the coil to keep it positioned. The heating element leads were positioned so that they extended out through another fused silica tube that served as a thermal radiation shield. This tube was partially coated with a high temperature fusable ceramic gold overglaze. The tubes were held together with endcaps made of a castable ceramic refractory. Clamping of the element leads held the furnace in place (Fig. 7).

We experienced frequent breaking of the Pt coils, and they quickly became so embrittled that they were unusable. This is due to the high temperature crystal growth of Pt. When we realized that this was happening we started using W-26Re wire for the heating element. Subsequent experiments with this heating element material were much more productive.

The second type of furnace [Aldrich, 1982, NASA/MSFC, personal communication] (Figs. 8 and 9) used in this study consists of a W-26Re heating element coiled around an alumina tube and embedded in an alumina cement. This isothermal furnace is open on the bottom to permit the samples to drop through the furnace, and a mirror is provided to observe the droplets that form. The furnace has Mo foil radiation shielding to reflect thermal radiation and is water-cooled. For both furnaces a pneumatic line is run through the top of the furnace and connected to the ceramic crucible.

Several different sample crucible configurations were used to contain the molten alloy prior to dripping down the drop tube (Fig. 10). The first crucible type consisted of alumina tubes 7 mm od and 4.5 mm id with one end sealed. A carbon dioxide, laser-drilled orifice 0.3 mm in diameter was burnt in the sealed bottom. Upon dropping samples, we discovered that the molten droplets were too large to solidify in the 2.4 s available with the 100-ft drop tube. The large size droplets resulted because the molten metal wetted the bottom of the crucible. We made several modifications in an attempt to form smaller droplets. One approach was to coat the crucible tip with graphite in an organic slurry. The crucible was then dried at 400°C. It was thought that the surface tension of the graphite would help prevent the droplets from adhering to the crucible. This did not work; the droplets continued to wet the crucible forming large droplets that splatted upon reaching the bottom. Another approach was to attach a 2-mm-diameter alumina rod to the end of the crucible. This was sometimes useful for forming smaller droplets. If the droplet of molten alloy flowed out of the orifice and wetted the rod, then it would run down the rod and drip from the much smaller end of the rod. One other approach was tried. A hole 1.5 mm in diameter was drilled in the bottom of the crucibles, and a hollow alumina tube 1.5 mm od and 0.5 mm id was inserted into the hole and cemented in place with a refractory cement. Although the small diameter tube very frequently clogged, we were able to eventually produce a number of droplets from 0.5 to 3 mm in diameter.

Quartz capillary tubes were also investigated. Although fused silica tubes are useful for certain alloys, they could not be used with $NiAl_3$. In all cases the molten metal reacted quickly with the silica sealing the orifice.

A sample of either the prealloyed powder of nominal 25% Ni-75% Al composition (in atomic %) or the containerlessly premelted slug was placed into the crucible. A range of powder weights from 0.1 to 1 g of the alloy was used. The orifice diameter of 0.3 mm was chosen since it was the largest diameter hole that would not let the metal powder pour out.

In other experiments the $NiAl_3$ samples were charged into the crucibles as premelted pellets. An alumina rod (0.25 in. diameter) and aluminum die assembly was constructed to press the powder. About 0.3 g of powder was weighed and poured into the press. A Carver press was used to supply a load of about 2000 lb. This was about the maximum load that could be applied with the alumina assembly. The pressing pressure calculates to be about 10,200 psi. The pressed pellet was levitation-melted with a laboratory electromagnetic levitation (EM) furnace in a vacuum chamber (Fig. 11) that was pumped to a vacuum of about 1 Torr and backfilled to about 100 Torr with Ar. Figure 12 illustrates the thermal history of one of these samples. As the sample was levitation-melted, one could see islands of impurities on the surface of the molten sample. These impurities appeared dark when compared with the molten metal. With repeated melting and quenching with a jet of H_2-5% He gas, the impurities seemed to coalesce together so that there were large patches of impurities after an hour or two of melting. This sample happened to produce one of the most successful drops. Upon removal of the samples from the EM levitator, it was found that the surface impurities formed a loose powder that was easily removed from the sample by light brushing. Other oxides were much more tightly bound to the surface. It happened that nearly all of the surface contamination resided on the bottom third of the sample. This portion was removed by sawing the sample with a diamond waffering saw. Each electromagnetic induction levitation-melted sample was sliced into parts for use in several drop tube runs.

One other approach was taken in order to attempt to remove surface oxides from the premelted samples. A few samples of powder were melted under a flux with a composition of 40% NaCl, 40% KCl, 10% AlF_3, and 10% Na_3AlF_3 on a weight basis (melting point of 650°C). Premelted slugs were also pretreated with molten flux. Instead of cleaning the surface, the flux made the surface very black. The powders also did not seem to consolidate and the drop tube runs were unsuccessful.

The furnace assembly was mounted inside the bell jar on top of the drop tube and the sample processing initiated. The first time each furnace was used it was outgassed by heating to about 1000°C. During the outgassing of the Aldrich furnace, we typically saw the vacuum in the drop tube bell jar rise from about 2×10^{-5} to 1.2×10^{-4} at the higher bakeout temperatures. This rise in vacuum occurred while the turbomolecular pumps were running.

Prior to each drop tube run, the entire bell jar drop tube assembly was evacuated to about 1×10^{-4} Torr and backfilled to about 300 Torr with a dry He-5% H gas mixture about three times. An estimate of the leak rate of the drop tube was obtained by pumping down to 2×10^{-4}, turning the vacuum pumps off and watching the rise in pressure. After about 30 s the pressure rose to 5×10^{-4}. After the final pumpdown the drop tube was backfilled to slightly greater than atmospheric pressure for the experiment. The furnace was then heated at a rate of about 100°C/s to a final temperature of 1450°C to melt the alloy. After a 10- to 15-min soak at temperature, the pressure behind the ceramic crucible was slowly increased. For successful runs a difference in pressure between the bell jar and the crucible of 60 mm resulted in samples being squeezed out of the orifice in the bottom of the crucible. The samples then dropped from the crucible and were removed from the catcher at the bottom of the drop tube. In those cases when drops did not come out of the crucible, a backpressure as high as 30 psi would not eject sample from the crucible.

The drop tube has a photovoltaic detector mounted in the drop tube just under the bell jar (Fig. 13). Whenever drops were observed the detector was activated to record a signal that was proportional to the brightness of the sample. The signal naturally decreases in intensity as the sample falls away from the detector and cools. If solidification is rapid enough and the heat liberated by the latent heat of fusion is sufficiently large, then a peak is observed in the intensity versus time signal from the detector. From the time of recalescence, the sample temperature can be estimated using a mathematical model and computer program designed to calculate the cooling of falling spheres due to combined convective and radiative cooling [13].

Some samples were examined with a JEOL U3 scanning electron microscope at 10 kV with Kevex Energy Dispersive X-Ray Analysis (EDXA). Other samples were sliced with a diamond waffering saw and mounted for light microscopy. They were polished through a series of SiC papers followed by 0.3 and 0.5 μm slumina powder. The polishing was done in alcohol to prevent the etching of the Al-rich phases. The samples were etched with water. A Carl Zeiss microscope was used to take light micrographs.

RESULTS

The results from the drop tube runs with the $NiAl_3$ samples are summarized in Table 1. This table gives a description of each of the drop tube experiments including the form in which the initial sample was prior to processing, the experimental parameters. the particular furnace and crucible used, the weight of the sample, and a comment on the results. It was often difficult to consolidate the molten alloy droplets due to the Al oxide dross on the surface of each of the $NiAl_3$ particles in the powder. The oxide skin on each particle apparently kept the molten droplets from wetting one another and prevented consolidation of the molten particles in a large number of drop tube runs. Figure 15 is a scanning electron micrograph of one of these samples that did not consolidate. The size of the particles in Figure 14 is roughly the same as the features in Figure 15, indicating that the features in Figure 15 are artifacts from the original surface scale. Heating to temperatures in excess of 1500°C in the reducing environment of the 5% H gas often did not seem to aid the consolidation. Application of a large backpressure (30 psi) behind the crucible was effective in only a few sample runs, permitting the formation of 0.5- to 4-mm diameter spheres.

Sample runs using electromagnetic levitation-melted starting samples were much more successful in producing drops than were the powdered samples. Prior to the drop tube melting, the individual particle surface films were consolidated and could be removed from the surface of the samples. Several of the most successful runs were achieved with these samples.

Theoretical cooling rates for spheres of several diameters were calculated using a computer model developed by Robinson [1983, NASA/MSFC, personal communication] and a computer program named NEWSPH written by Robinson for the HP 9835 computer. This program uses a solution to a differential equation containing radiative and convective cooling terms. Materials properties for Al and Ni were obtained and values for $NiAl_3$ estimated from an ideal average of Ni and Al. Table 2 gives the values used. Cooling curves were calculated for psheres of 0.5, 0.2, 0.1, 0.05, and 0.02 cm in diameter, falling in 760 Torr He, and are shown in Figure 16.

Samples of several types were obtained (Fig. 17) including spheres, splats, and a few needles. The needles were probably produced as the last liquid in the crucible was expelled by the backpressure in the crucible. All of the spherical samples and the needles have rough dendritic surface features; see Figures 18 and 19. The splatted samples have more unusual surface features as illustrated in Figure 20.

Figure 21 is the published phase diagram [14] for the Al-Ni system. As can be seen in this figure, for a liquid with a 75 percent composition of Ni, the first phase to solidify is Ni_2Al_3. As the sample cools further, $NiAl_3$ forms from about 854°C to about 640°C. The last liquid to solidify forms the eutectic mixture of Ni and $NiAl_3$. Figure 22 is a light micrograph of a small ingot of Al-Ni alloy with a nominal composition of $NiAl_3$. The dark region is the Ni_2Al_3 phase. Surrounding this phase is $NiAl_3$. The speckled regions between these grains represent the eutectic mixture.

Most of the drop tube samples retrieved from the sample catcher were found to be spherical in shape with rough dendritic surface features much like the 9 mm Cu and 6 mm Ag said to be "containerlessly solidified" in space by Zemskov et al. [15]. The SEM micrographs of Figure 18 are typical of the surface of the spherical samples. One can see the dendritic surface characteristic of alloys rapidly solidified in free fall. The primayr surface dendrite arm spacings range from about 5 μm for the small sphere (0.65 mm) to about 30 μm for the larger sphere (1.7 mm). Figure 23 illustrates light micrographs of other drop tube-solidified samples. One can see that the microstructure is very similar to that of the small ingot sample in Figure 22. There are considerable regions of Ni_2Al_3 surrounded by the desired $NiAl_3$ phase. Again the eutectic phase fills the remaining volume.

Light micrographs of samples quenched by various techniques are shown in Figure 24. There is a large variation in the scale of the microstructural features. This is also evident in Figure 23 which compares various containerlessly solidified samples. In comparison, Figure 25 illustrates the microstructure of splatted samples.

Figure 26 is a plot of the Dendrite Arm Spacing (DAS) versus cooling rate for $NiAl_3$ published by Brooks et al. [16]. This data can be used to estimate the cooling rates that were obtained with the drop tube-solidified samples. DAS was measured on a number of light micrographs calibrated with a micrometer slide. For each sample, a range of DAS values was obtained and an average value calculated. The results are plotted as circles in Figure 26. The electromagnetic-levitated sample has an average DAS of 10 to 40 μm, indicating an effective cooling rate of about 10 to 30°C/s. In contrast, the rapidly solidified 0.22-mm-diameter needles have a DAS of about 1 to 2 μm with a respective cooling rate of over 20,000°C/s.

DISCUSSION

In other drop tube solidification studies investigators have successfully undercooled Nb and NbGe alloys well below their melting points. Also, a glass forming alloy of PdSiCu with a reduced glass temperature (Tg/Tm) of 0.64 has been solidified to the amorphous state. Since drop tube containerless solidification has been a successful technique for undercooling these alloys, the current work was undertaken to

utilize this technique to investigate the formation of a new microstructure in Ni-Al alloys. The original goals of the study was to undercool molten Ni-Al alloy (with 25% Ni) below the peritectic temperature so that a larger fraction of the $NiAl_3$ phase might be formed.

Observation of large volume fractions of Ni_2Al_3 in Figures 23 and 24 indicate that we did not achieve any significant difference in the proportions of alloy components with any of the various solidification processes. Most importantly, we did not seem to form any more of the $NiAl_3$ phase or any less of the Ni_2Al_3. All microstructures indicate that the normal routes to solidification apply for all the containerlessly solidified samples. That is, crystallization began at a temperature between the point on the liquidus 1100°C and the peritectic temperature 854°C. The first phase to solidify was Ni_2Al_3. As Ni_2Al_3 grew in the liquid, the composition of the remaining liquid followed the liquidus line on the phase diagram to the peritectic temperature. Below 854° to 640°C, $NiAl_3$ is the thermodynamically stable phase that solidifies. The presence and location of large proportions of Ni_2Al_3 substantiates that the sample temperature was above the peritectic temperature when nucleation occurred.

Nucleation appears to have started at the surface. Figure 27 shows a cross section of a 0.65 mm sample. One can see the dendrite arms that grew through the sample. Since crystallization releases latent heat of fusion reheating the sample (increasing the DAS), one can assume that the most rapid solidification (smallest DAS) occurs at the initial onset of nucleation. This corresponds areas with the finest dendrite arm spacing. Tracing the dendrite arms, it appears that, in general, they originated at the surface of the sample.

In undercooling studies of Al in molten NaOH, the maximum amount that Turnbull and Chen [8] were able to undercool Al was less than 130°C. They indicated that when the NaOH flux was not used, the most that Al could be udnercooled was about 40°C. Turnbull and Chen speculated that Al oxide on the sample surface was responsible for the heterogeneous nucleation of crystallziation preventing significant undercooling.

More recently, Rasmussen [1983, Clarkson Institute of Technology, personal communication] has been able to extend the undercooling limit to about 150°C for an Al-Si alloy. When compared with metals such as Ga, these undercooling values are a small fraction of the absolute melting temperature. Examination of the free energy of formation of metal oxides versus temperature [17] indicates that Al_2O_3 is a very stable oxide. The use of H as a reducing gas is of little use in breaking down the Al_2O_3 that has already formed. Since there was no way for the oxide to have been removed from many of the samples, one can assume that Al_2O_3 was present in all of the drop tube samples. Figure 28 shows what appears to be a portion of the original Al_2O_3 dross from the sample surface of one of the drop tube samples. Energy Dispersive X-Ray Analysis (EDXA) shows that it is primarily Al oxide (Na, Si, S, and Cl are artifacts of handling) (oxygen cannot be detected by EDXA).

Another unsuccessful set of experiments involved the drop tube solidification of a Cu-Zr alloy. It was postulated that if PdSiCu samples could be undercooled to amorphous alloys, then it should be possible to also form the amorphous Cu-Zr alloy. A measure of the glass forming ability of an amorphous alloy is the reduced glass

temperature (glass transition temperature/liquidus temperature). For the two alloys, CuZr and PdSiCu, the reduced glass temperatures are both 0.64 [18]. The unsuccessful attempts to form amorphous Cu-Zr may also be due to the presence of surface oxides such as ZrO_2 (another very stable oxide). The fact that we did not solidify appreciably more of the $NiAl_3$ phase with the drop tube samples than we did with the bulk casting or with the oil quenching indicates that we did not realize our desire to significantly undercool the samples in free fall. Drop tube containerless solidification does not necessarily produce the desired results of large degrees of liquid undercooling. Surface reaction films left over from the original sample or produced during the free fall solidification may act as effective heterogeneous nucleation catalysts.

CONCLUSIONS

A "dripper furnace" procedure has been developed which facilitates the formation and containerless solidification of small diameter metal alloy spheres utilizing the MSFC drop tube facilities. The process overcomes sample size limitations inherent in electromagnetic levitation and electron beam techniques. Sample diameters as small as 0.5 mm were produced by the process.

The production of $NiAl_3$ alloy with predominately single phase $NiAl_3$ by undercooling the alloy $NiAl_3$ below the peritectic before solidification does not appear feasible using the MSFC drop tube facility as presently configured. The results of this containerless solidification study as well as those of previous studies using NaOH flux and fine dispersions indicate that aluminum metal is prevented from undercooling more than about 150°C below the liquidus by heterogeneous nucleation from Al_2O_3 on the surface of the sample. While PdSiCu and Nb-Ge alloys, which have much less stable oxides, have been undercooled to unprecedented levels for bulk samples using containerless drop tube solidification, samples of $NiAl_3$ and Cu-Zr which have extremely stable oxides under the same experimental consideration of oxidation/reduction properties of candidate drop tube specimens is imperative. More data on maximum undercoolings for elemental materials in the drop tube would be helpful for planning subsequent experiments.

Containerless solidification of $NiAl_3$ in the drop tube resulted in samples from less than 0.5 mm to several mm in diameter in spherical and sometimes needle form. Cooling rates obtained in this study, determined from published dendrite arm spacing data, ranged up to 20,000°C/s. The containerlessly solidified samples exhibited a number of interesting surface morphologies possibly unique to containerlessly processed samples, some of which were similar to larger metal samples containerlessly processed in space.

REFERENCES

1. Brown, R. L. and Zoller, L. K.: Avenues and Incentives for Commercial Use of a Low-Gravity Environment. NASA Technical Paper 1925, 1981.

2. Baird, M. J. and Steffgen, F. W.: Methanation Studies of Nickel-Aluminum Flame Sprayed Catalysts. Ind. Eng. Chem., Prod. Res. Dev., Vol. 16, 1977, pp. 142-147.

3. Fasman, A. B., Timofeeva, V. F., Rechkin, V. N., Klyuccnikov, Yu. F., and Sapukov, I. A.: Effect of the Composition of a Nickel-Aluminum Alloy on the Structure and Specific Activity of a Raney Nickel Catalyst. Kinetics and Catalysis (USSR), Vol. 13, 1972, pp. 1347-1352.

4. Oden, L., Sanker, P., and Russell, J. H.: Method for Producing Supported Raney Nickel Catalysts. U. S. Patent 4,049,580, 1977.

5. O'Hare and Mauser, J. E.: Bureau of Mines Report No. 8210, 1977.

6. Stiles, Alvin B.: Activated Nickel Catalysts. U. S. Patent 3,627,790, 1971.

7. Petrov, B. E., Cherkashina, N. V., Fasman, A. B., Sokolskii, D. V., Lebedeva, N., and Baraovashina, E. P.: Kin. t. Katal. Vol. 19, 1969, p. 1146.

8. Turnbull, D. and Cech, R. E.: Microscopic Observation of the Solidification of Small Metal Droplets. J. Appl. Phys., Vol. 21, 1950, pp. 804-810.

9. Perepezko, J. H., and Paik, J. S.: Undercooling Behavior of Liquid Metals. In Rapidly Solidified Amorphous and Crystalline Alloys. B. H. Keer, B. C. Giessen, and M. Cohen (editors), Elsevier Press, New York, 1982, pp. 49-63.

10. Lacy, L. L., Robinson, M. B., and Ratz, T. J.: Containerless Undercooling and Solidification in Drop Tubes. J. Crys. Growth, Vol. 51, 1981, pp. 47-60.

11. Robinson, M. B.: Undercooling Measurement in a Low-Gravity Containerless Environment. M.S. Thesis, U. of Alabama, Huntsville, 1981.

12. Steinberg, J., Lord, A. E., Jr., Lacy, L. L., and Johnson, J. J.: Production of Bulk Amorphous Pd-Si-Cu in a Containerless Low-Gravity Environment. Appl. Phys. Lett., Vol. 38, 1981, pp. 135-137.

13. Robinson, M. B., and Wills, F. D.: Solution to the Differential Equation for Combined Radiative and Convective Cooling for a Heated Sphere with Applications. Submitted to J. Appl. Phys., Space Science Lab., Marshall Space Flight Center, NASA Preprint No. 83-127, 1983.

14. Willey, L. A.: Appendix 1. Phase Diagrams. In Aluminum-Volume I, pp. 359-381, K. R. Van Horn, editor, and Metals Handbook-Vol. 8, p. 262, Am. Soc. for Metals, 1967.

15. Zemskov, I. N., Belokurova, A. A., Savytchev, V. V., and Bogdanova, N. F.: Solidification of Copper and Silver Under Microgravity Conditions. J. Crystal Growth, Vol. 60, 1982, pp. 86-90.

16. Brooks, C. S., Lemkey, F. D., and Golden, G. S.: Rainy Type Catalysts From RSA Atomization of Al-Ni Powders. In Rapidly Solidified Amorphous and Crystalline Alloys, B. H. Keer, B. C. Giessen, and M. Cohen, editors, Elsevier Press, New York, 1982, pp. 397-407.

17. Richardson, F. D., and Jeffes, J. H. E.: J. Iron Stee' Institute, Vol. 60, 1948, p. 261.

18. Donald, I. W., and Davies, H. A.: Prediction of Glass Forming Ability for Metallic Systems. J. Noncry. Solids, Vol. 30, 1978, pp. 77-85.

TABLE 1. Al_3Ni Drop Tube Experiments

Sample	Date	Run No.	Experiment	Crucible	Furnace	Weight	Comment
Al_3Ni Powder	12-3-81	1	1700°C Bell Jar 3 ft drop oil quench	Al_2O_3 - 0.2 mm orifice	Aldrich	0.6 g	3 samples - 6.9 x 4, 5.2 x 7, 9 x 3 mm
"	12-3-81	2	"	"	"	0.6	No drops
"	12-9-81	3	"	"	"	0.6	No drops - no samples
"	12-14-81	4	1670°C "	"	"	0.5	2 drops - 3 x 5, 4 x 4 mm 1 stuck to furnace 3 x 5 mm
"	12-29-81	5	1675°C " " quench on glass	Al_2O_3 0.2 mm graphite coated	"	0.4	1 splat - 4 x 4 mm
"	12-29-81	6	1475°C " " Oil quench	"	"	0.4	1 drop 11 x 4 x 6 mm
"	12-30-81	7	1465°C "	"	"	0.18	3 drops - 2.5 x 2.4, 2.4 x 4, 2.5 x 4 mm
"	1-19-82	49	1450°C 100 ft drop tube 760 mm He-6% H	"	"	0.14	1 drop - needle, 2 spheres (0.52, 0.69 mm)
"	1-20-82	50	"	"	"	0.15	2 drops - computer date 1 splat, 5 spheres (1-2.5 mm), 1 needle
"	1-20-82	51	"	"	"	0.17	Did not drop down tube - splat on base plate, 3 spheres
"	1-21-82	52	"	"	"	0.15	1 drop - 1 sphere (2.5 mm) sample on tip of crucible
"	1-21-82	53	"	"	"	0.15	2 drops, hit wall of drop tube, splat. 1 sphere, 2 needles
"	1-21-82	54	"	"	"	0.15	2 drops - splat at bottom, splat in bell jar, 1 sphere in bell jar
"	1-21-82	55	1450°C 100 ft drop tube 760 mm He-6H	Al_2O_3 0.2 mm orifice	"	0.16	1 drop - splat on closed top gate valve, several spheres
"	1-22-82	56	"	"	"	0.6	Drops hit drop tube wall, splat
"	1-22-82	57	"	"	"	0.05	1 drop - 1 sphere 2.2 mm
"	1-24-82	58	"	"	"	0.05	No drops

TABLE 1. (Continued)

Sample	Date	Run No.	Experiment	Crucible	Furnace	Weight	Comment
Al_3Ni Powder	1-25-82	59	1450°C 100 ft drop tube 760 mm He-6H	Al_2O_3 0.2 mm orifice	Aldrich	0.06	No drops
"	1-25-82	60	"	"	"	0.05	No drops
"	1-25-82	60A	"	Quartz Capillary tube	"	0.03	Orifice sealed, back pressure ruptured crucible, furnace failed
"	1-25-82	61	"	"	Johnson-Pt	1 g	Sample stuck to outside of capillary tube, no drops
"	2-3-82	62	"	"	"	1 g	No drops
"	2-3-32	63A	"	"	"	1 g	No drops - reaction noted between melt and crucible, Pt wire broke
"	2-3-82	63B	"	"	"	1 g	No drops
"	2-4-82	63C	"	Al_2O_3, 0.2 mm Orifice, 1 mm rod	"	1 g	Pt coil broke
"	2-4-82	63D	"	"	Johnson-W	1 g	Drops - 4 spheres (1.4 to 1.7 mm), 2 needles, sample on tip of crucible, 2 shiny spheres
"	2-4-82	64	"	"	"	1 g	No drops
"	2-4-82	65	"	"	"	1 g	Many samples - 3 splats, 12 spheres (0.5 to 1.5 mm), Glob stuck to furnace, recalescence data
"	2-4-82	66	"	"	"	1 g	Samples - 2 spheres (0.7, 0.8 mm)
"	2-5-82	67	"	"	"	1 g	No drops
"	2-5-82	68	"	"	"	1 g	No drops
"	2-5-82	69	"	"	"	1 g	No drops

TABLE 1. (Concluded)

Sample	Date	Run No.	Experiment	Crucible	Furnace	Weight	Comment
EM Melted Al_3Ni	3-17-82	70A	1450°C 100 ft drop tube 760 mm He-6H	Al_2O_3, 0.2 m, Orifice, 1 mm rod	Aldrich	0.22	1 drop - splatted to a powder, sample on tip of rod
"	3-17-82	70B	"	"	"	0.05	No drops
EM melted with flux	3-17-82	70C	"	"	"	1 ϟ	No drops
EM Melted Al_3Ni	3-18-82	71	"	"	"	0.83	Spray - many small spheres (0.5-2 mm) about 70
"	3-18-82	72	"	"	"	1	No drops
"	3-31-82	73	"	"	"	0.115	Furnace failed
"	4-1-82	74	"	Al_2O_3 with 0.3 mm ID Al_2O_3 tube	Johnson-W	0.1	2 drops
"	4-1-82	75	"	"	"	0.105	No drops
"	4-2-81	76	"	"	"	0.1	No drops
"	4-15-82	77	"	"	"	0.25	No drops
"	4-16-82	78	"	"	"	0.5	No drops
"	5-7-82	79	"	Al_2O_3 with 0.6 mm ID Al_2O_3 tube	"	0.3	No drops - sample on end of tube
"	5-14-82	80	"	"	"	0.3	No drops
"	5-18-82	81	"	"	"	0.3	No drops

TABLE 2. THERMODYNAMIC VALUES USED FOR SAMPLE COOLING RATE CALCULATIONS

Parameter	Value
Initial Temperature	1723 K
Emissivity	0.1
Heat Capacity	0.28 Cal/g K
Heat of Fusion	90 Cal/g K
Liquid Density	4.2 g/cc
Gas Pressure (He)	760 Torr
Final Temperature	1173 K
Sample Diameters	0.1, 0.2, 0.5, 1, 2, 5 mm

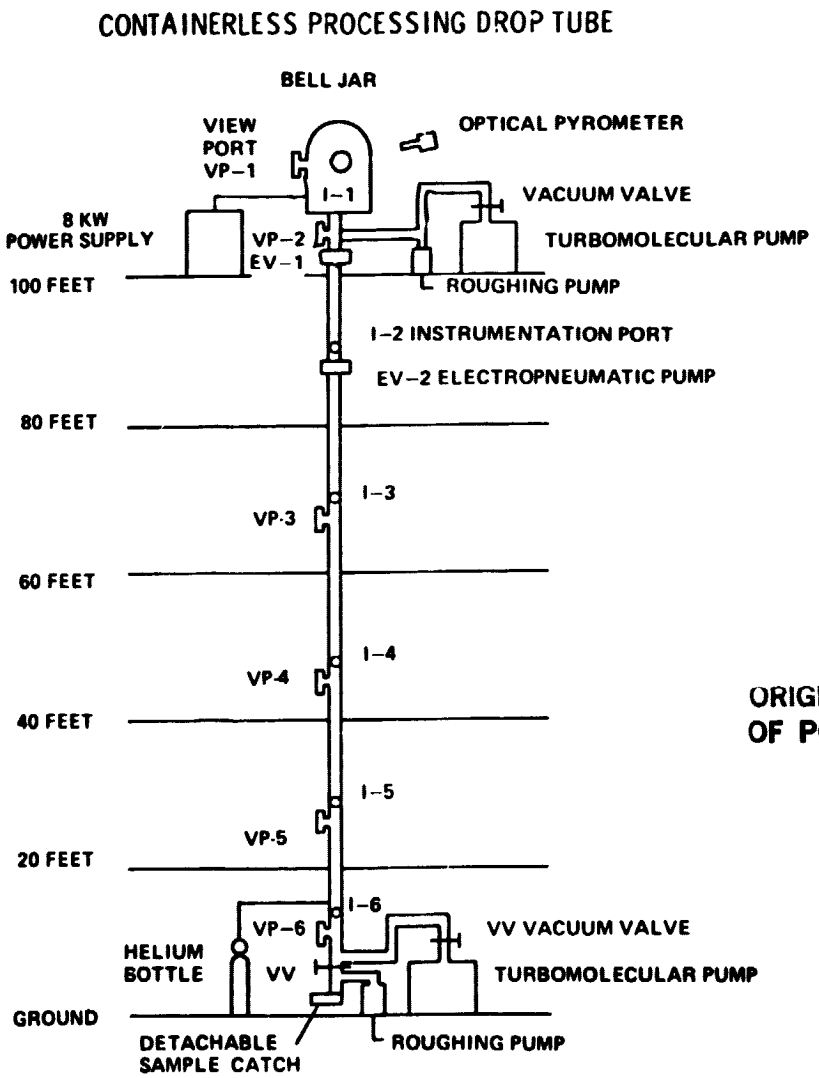

Figure 1. Schematic representation of the MSFC 100-ft drop tube.

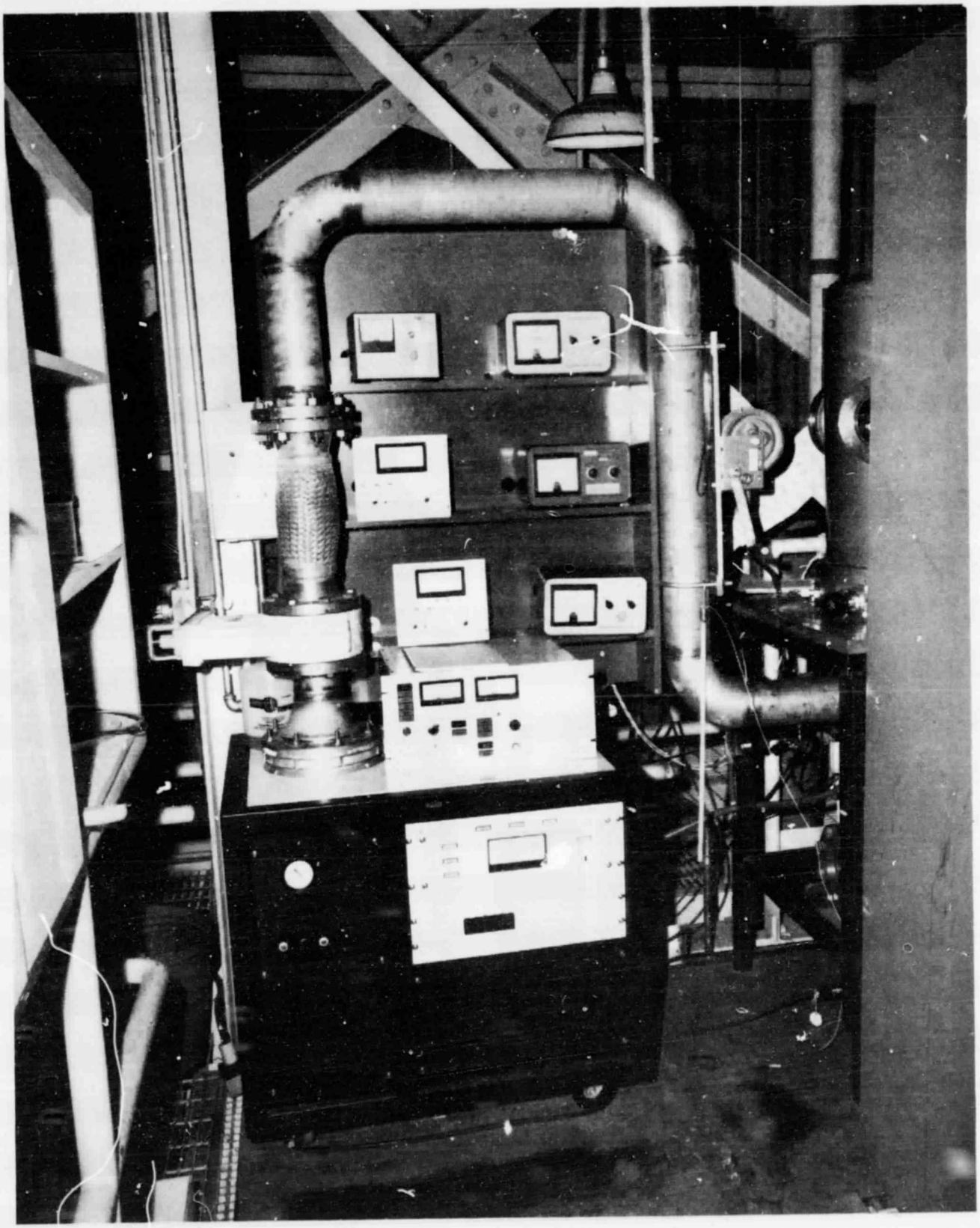

Figure 2. Photograph of the vacuum pump station and bell jar assembly at the top of the drop tube.

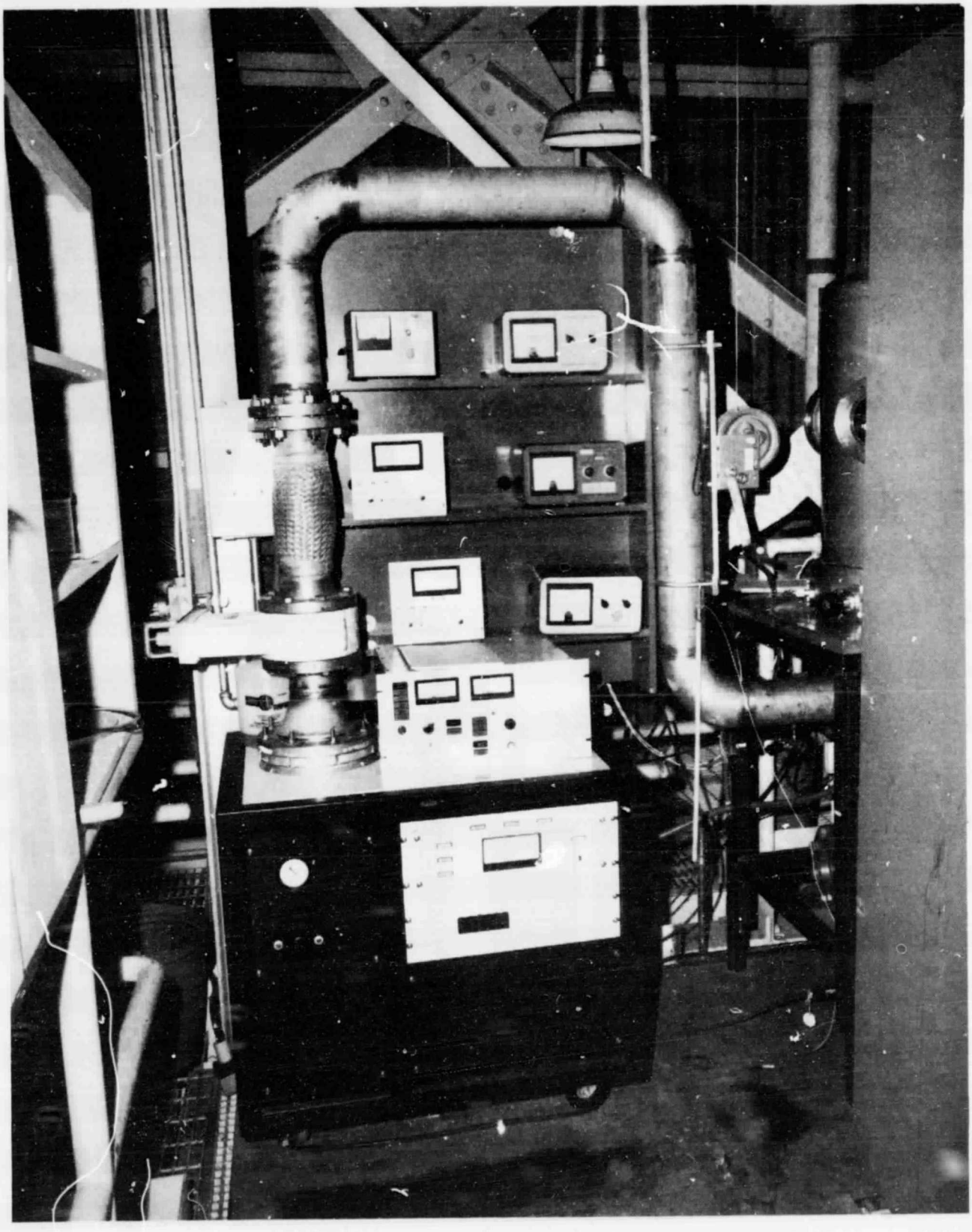

Figure 2. Photograph of the vacuum pump station and bell jar assembly at the top of the drop tube.

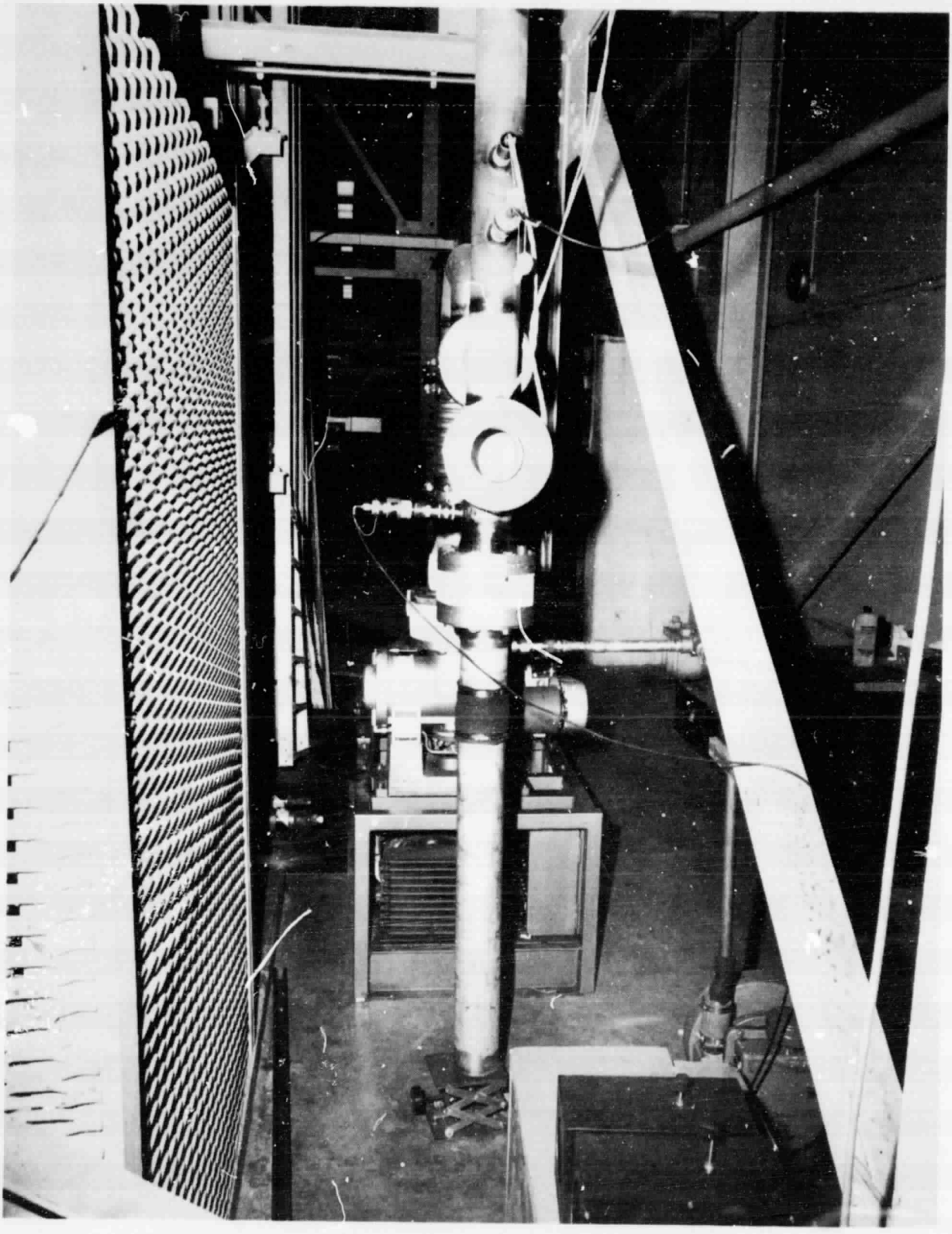

Figure 3. Photograph of the sample catcher and bottom pumping station.

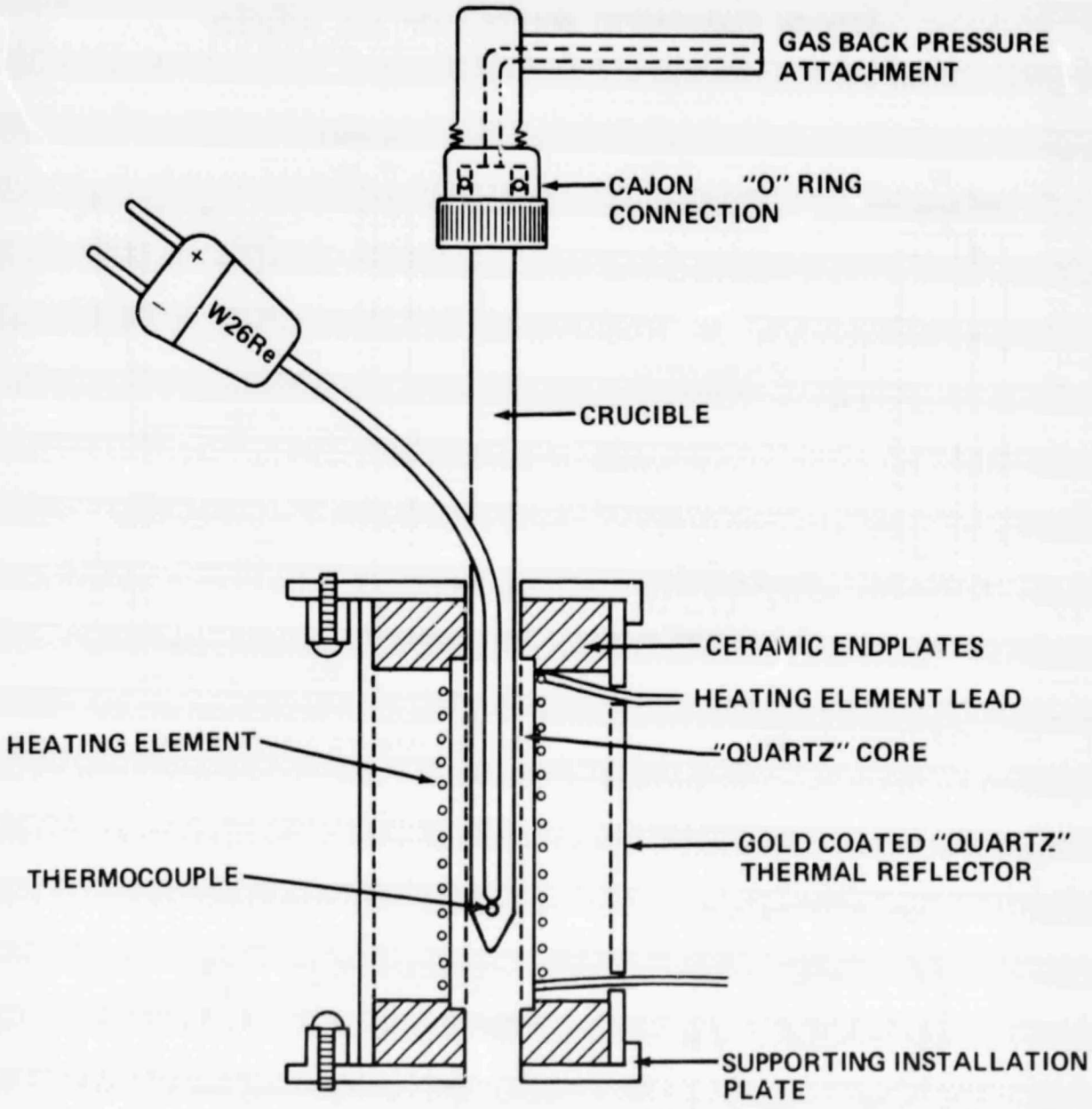

Figure 4. Schematic representation of the Johnson furnace.

JOHNSON TRANSPARENT QUARTZ DROP TUBE FURNACE

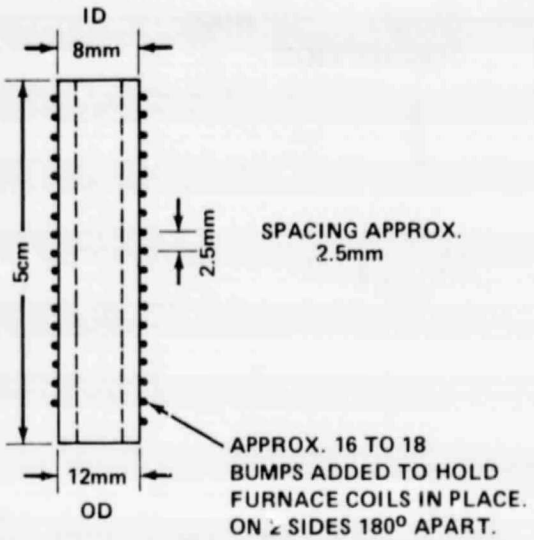

HEATING ELEMENT SUPPORT

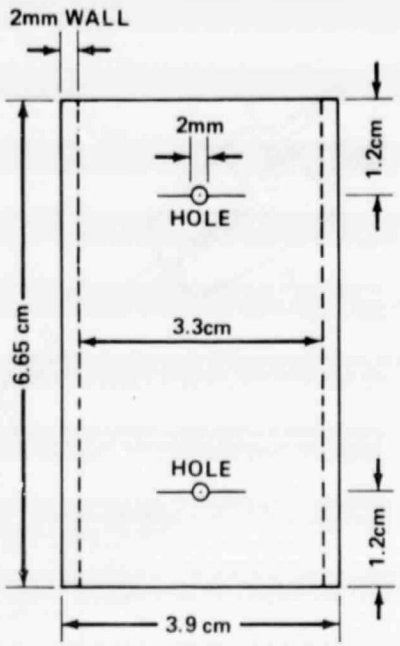

GOLD COATED QUARTZ THERMAL REFLECTOR

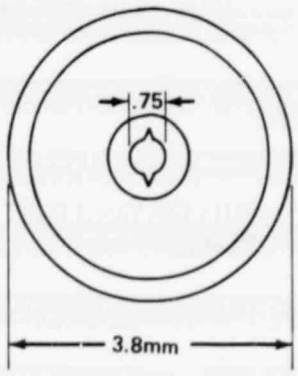

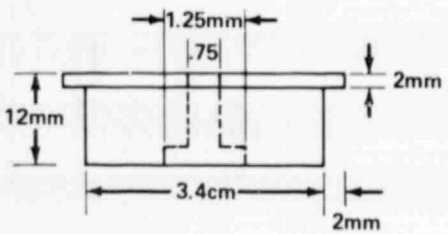

ENDCAPS

Figure 5. Drawings of the Johnson furnace components.

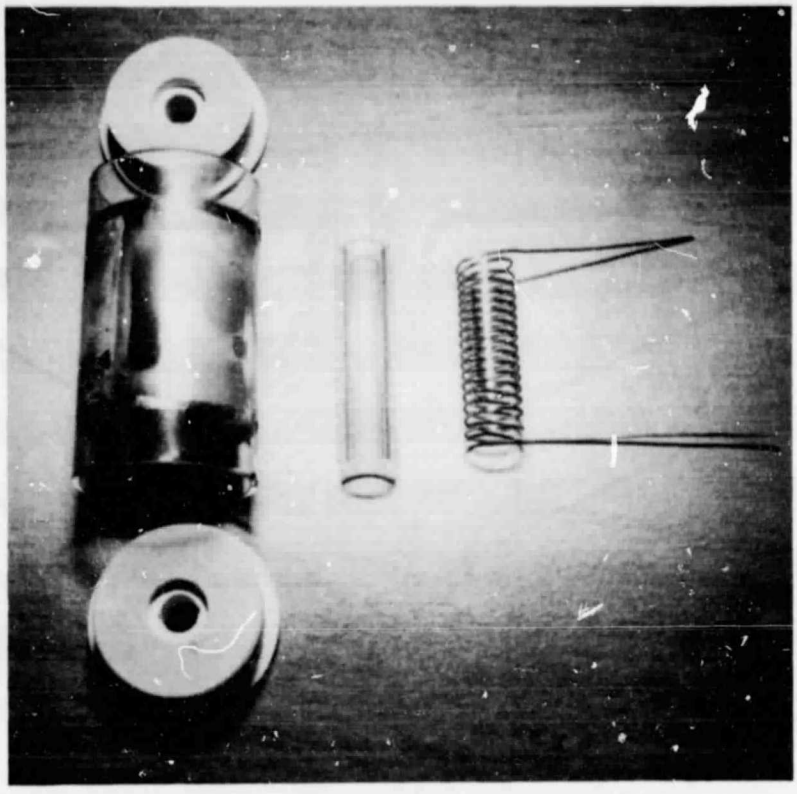

Figure 6. Photograph of the components of the Johnson furnace.

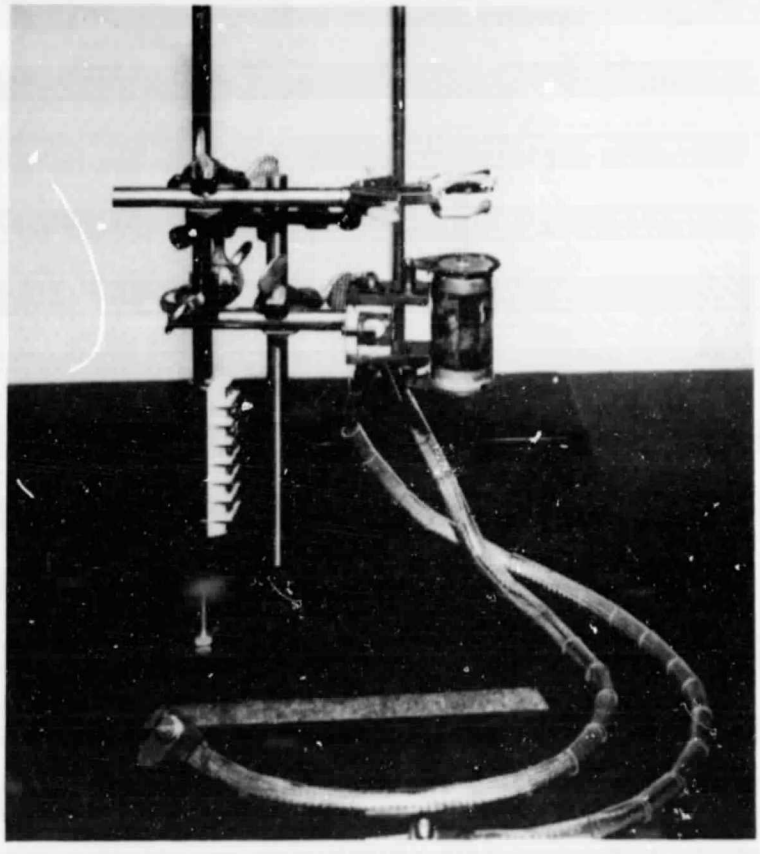

Figure 7. Photograph of the Johnson furnace as assembled.

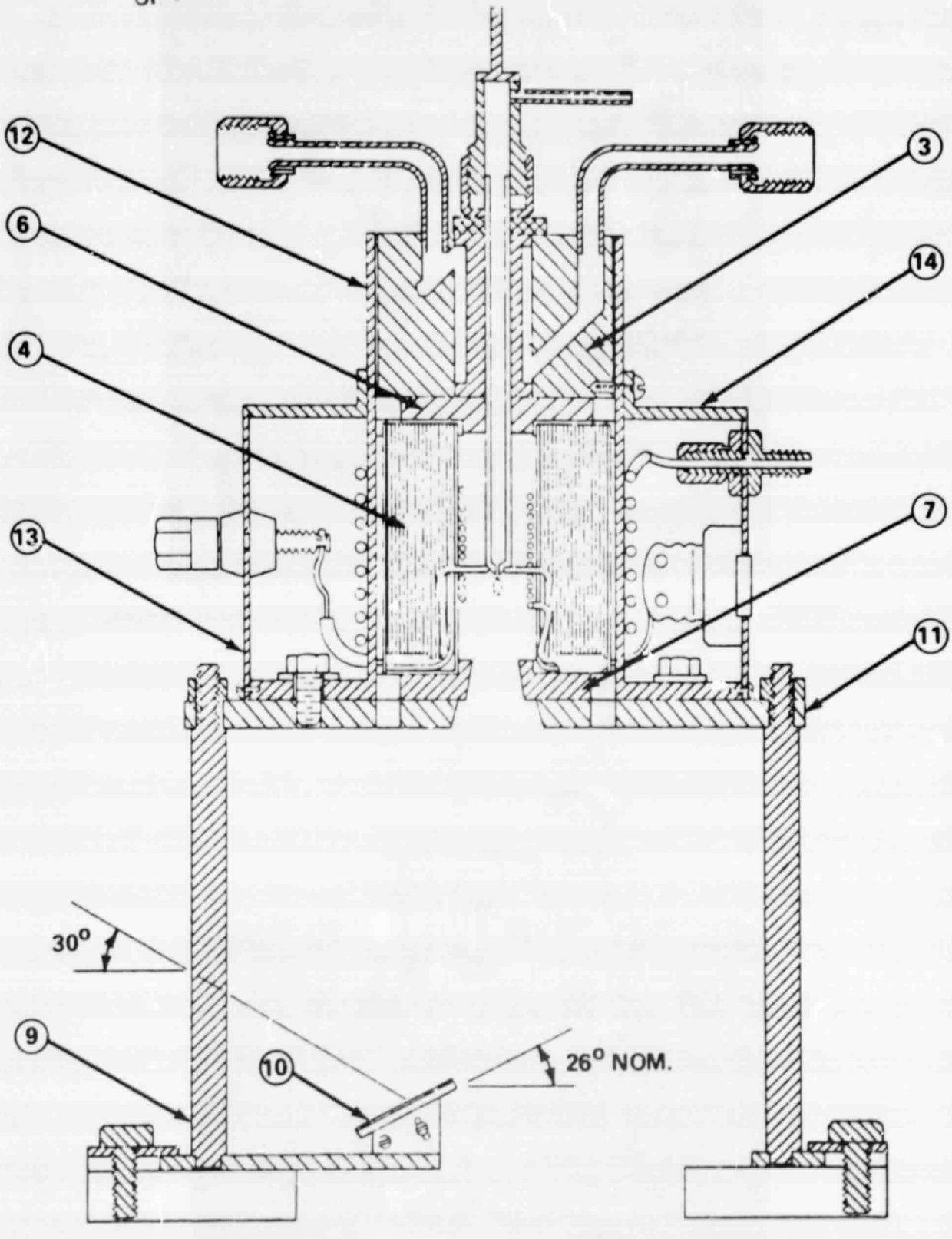

Figure 8. Schematic representation of the Aldrich furnace.

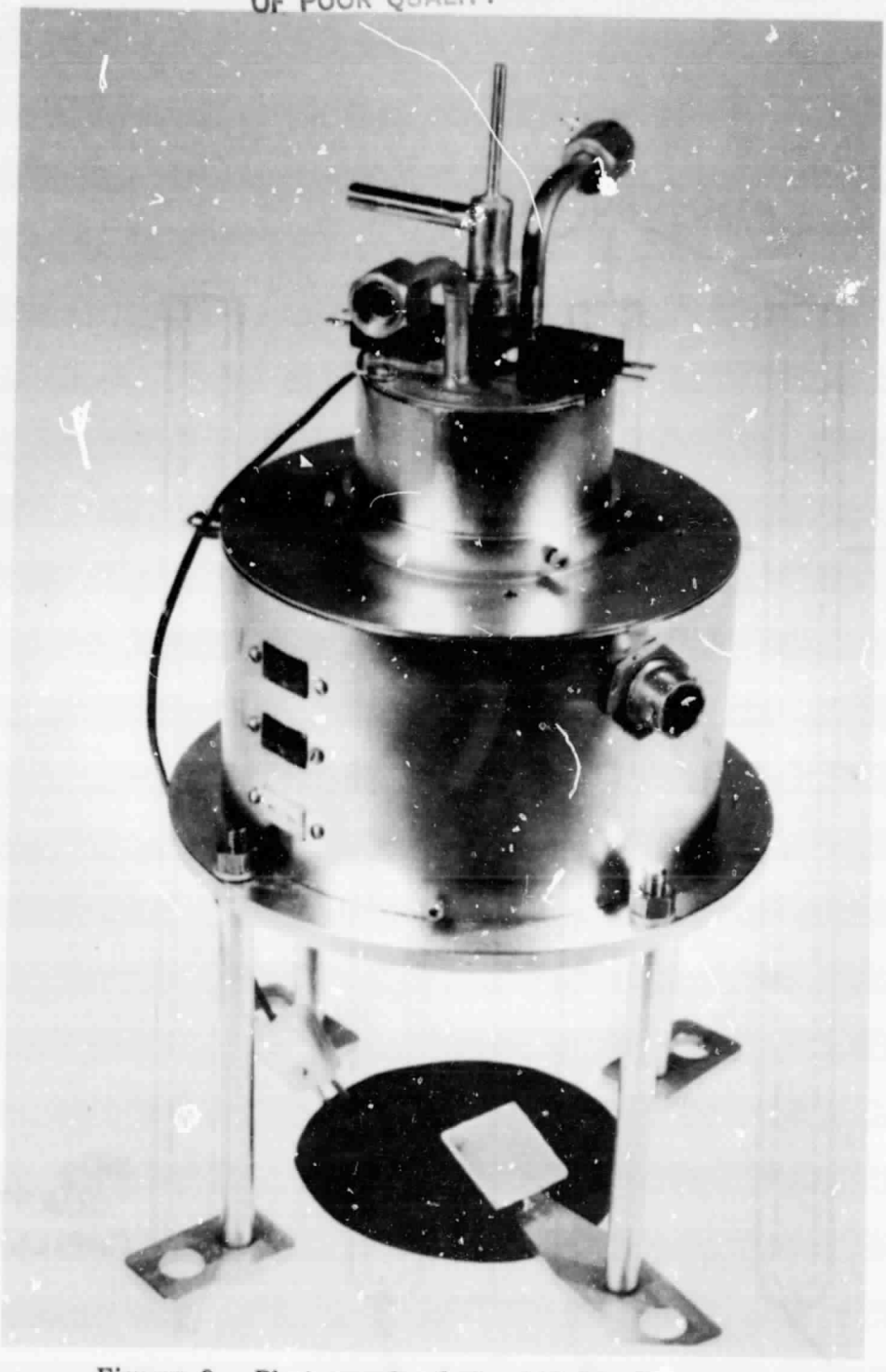

Figure 9. Photograph of the Aldrich furnace.

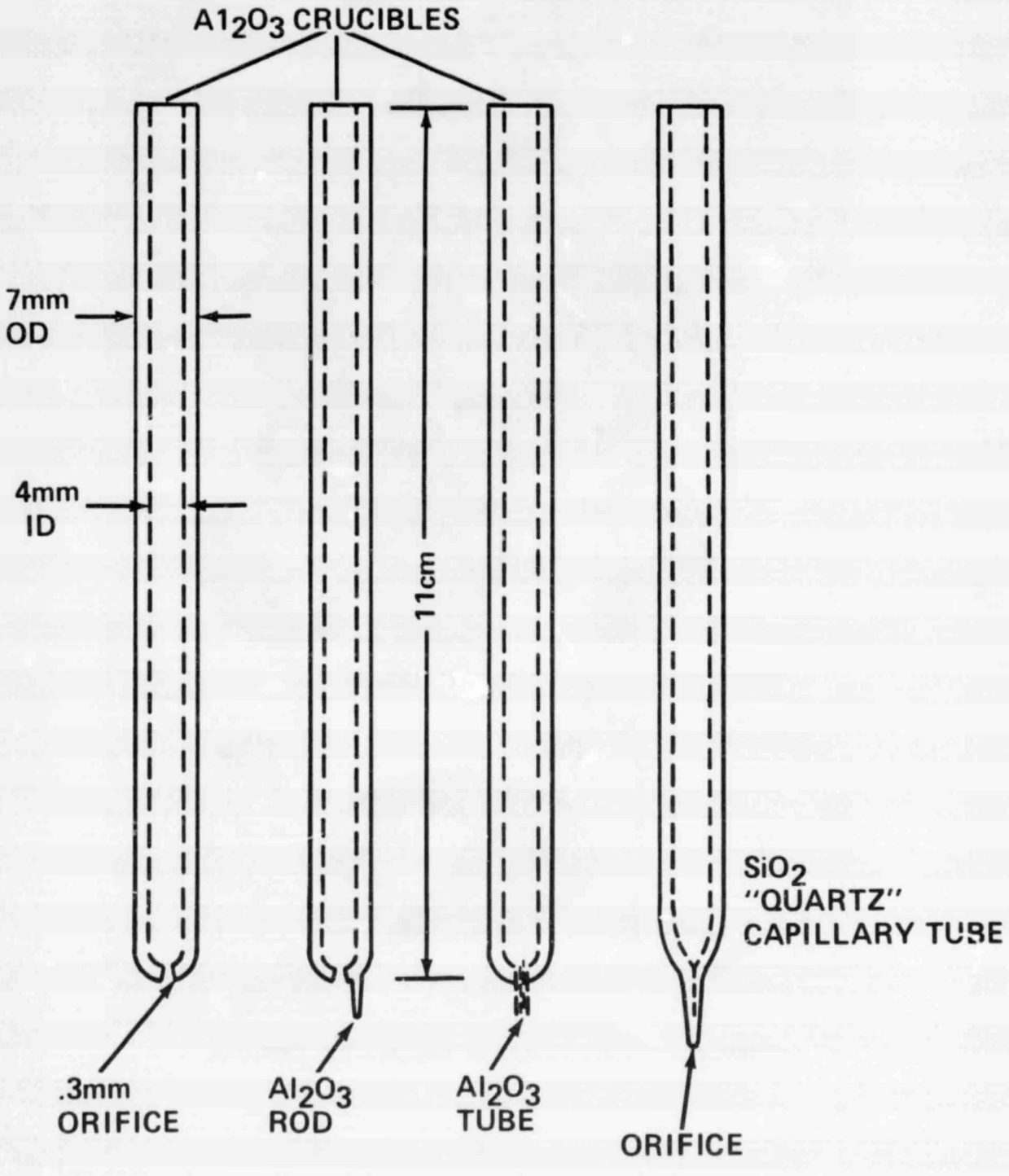

Figure 10. Schematic representation of the sample crucibles.

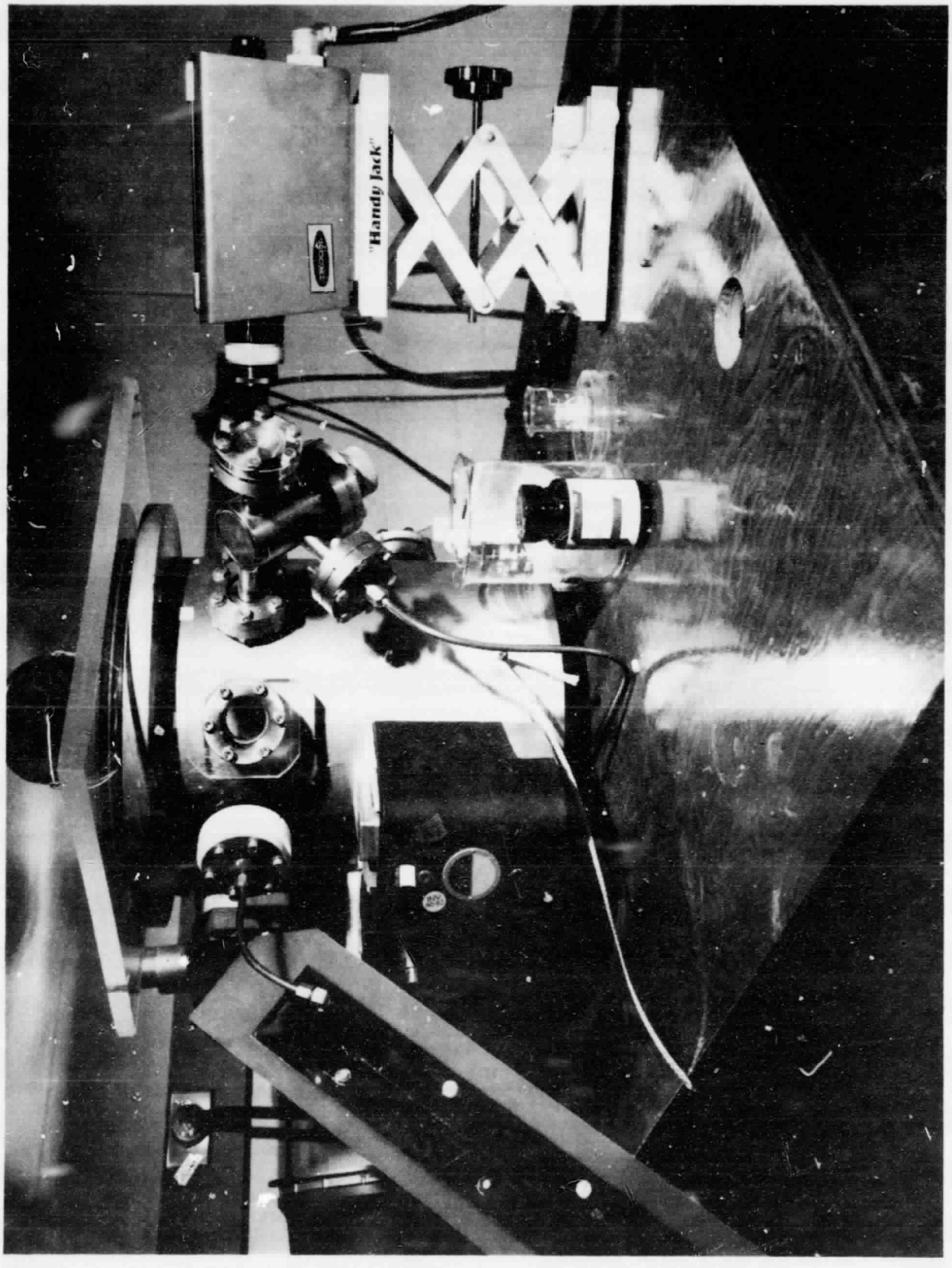

Figure 11. Laboratory containerless electromagnetic levitation processing facility.

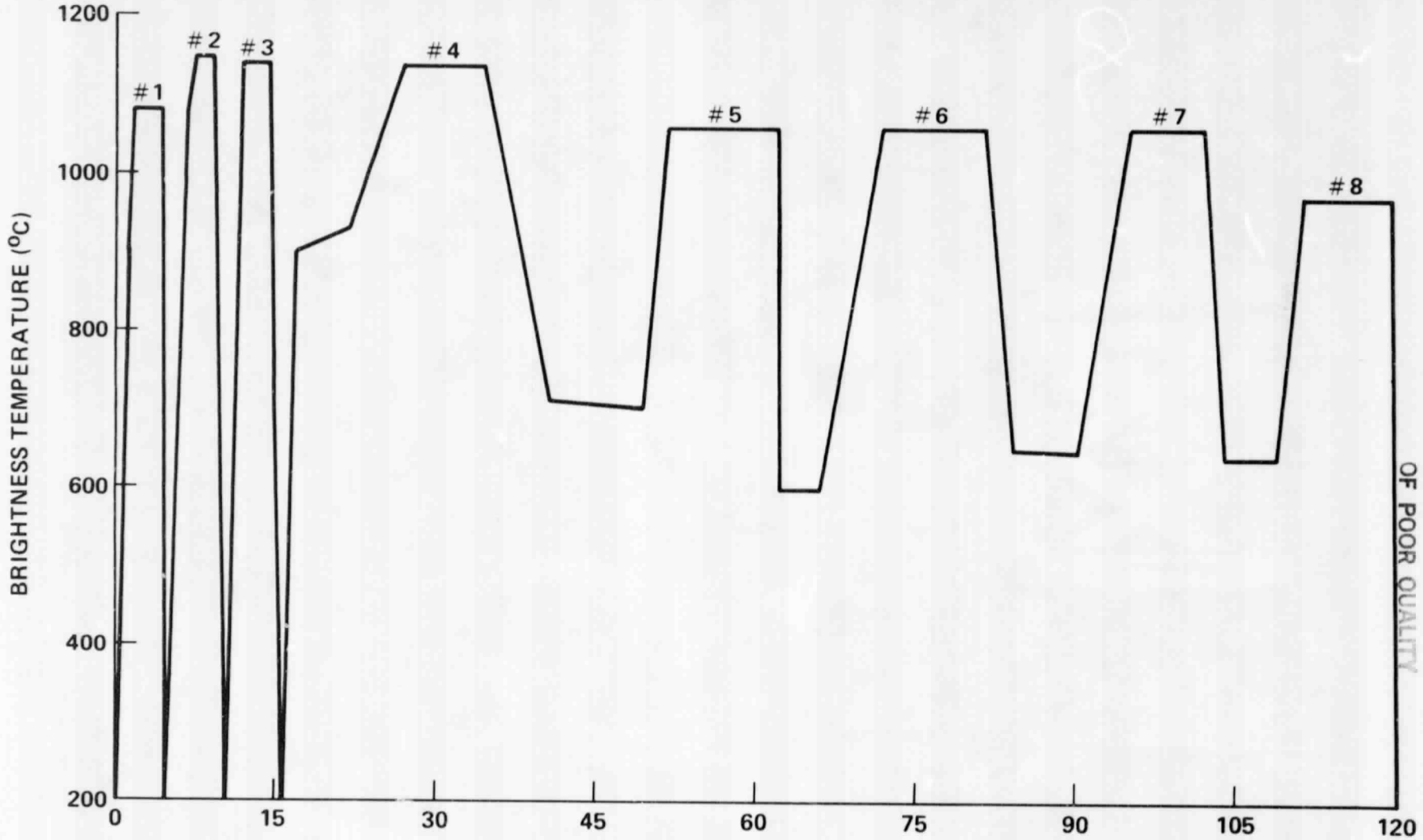

Figure 12. Thermal history of the conainerless electromagnetic levitation melted sample used from drop tube run 71.

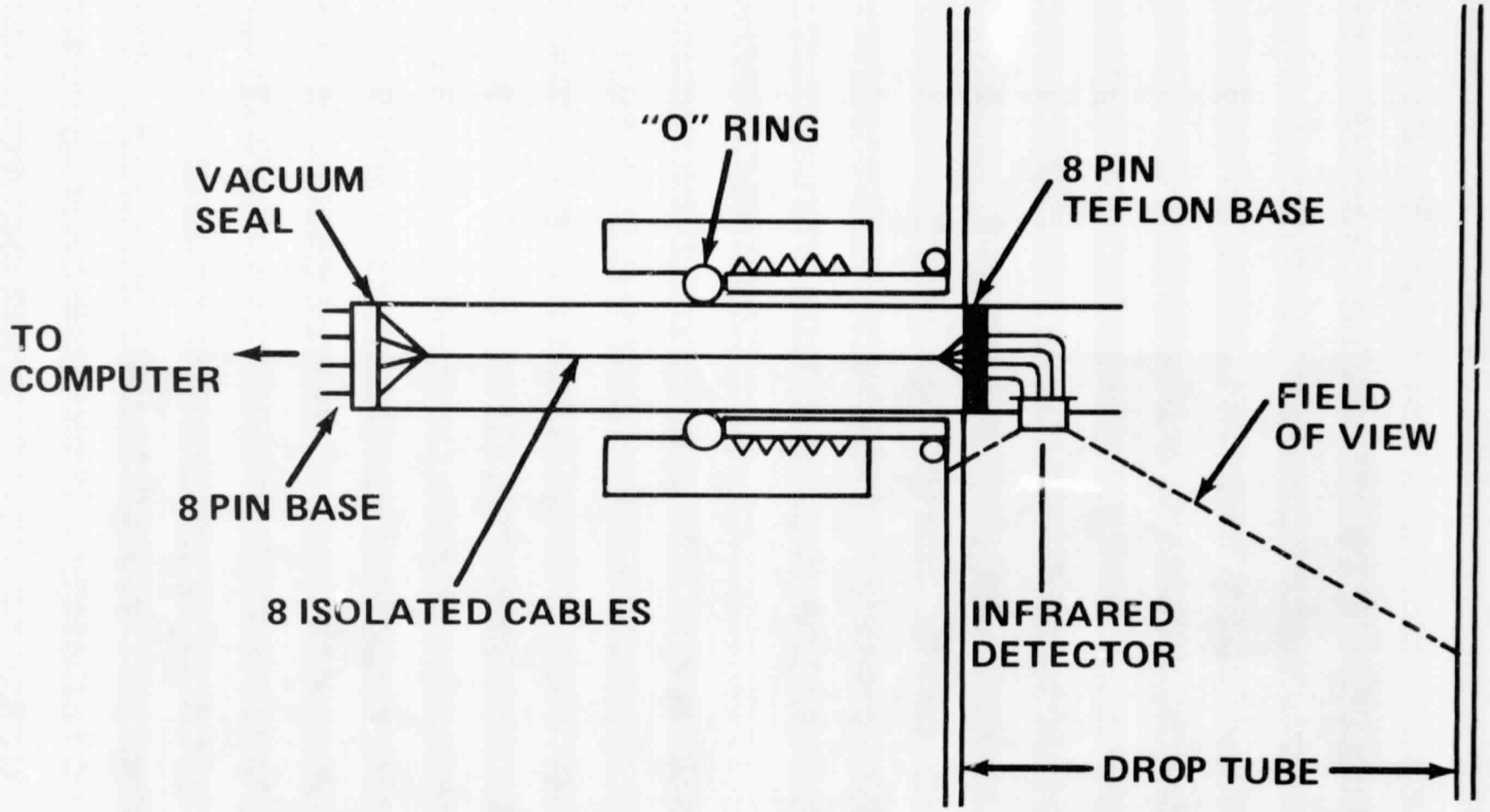

Figure 13. Schematic representation of the photocel installed in the drop tube.

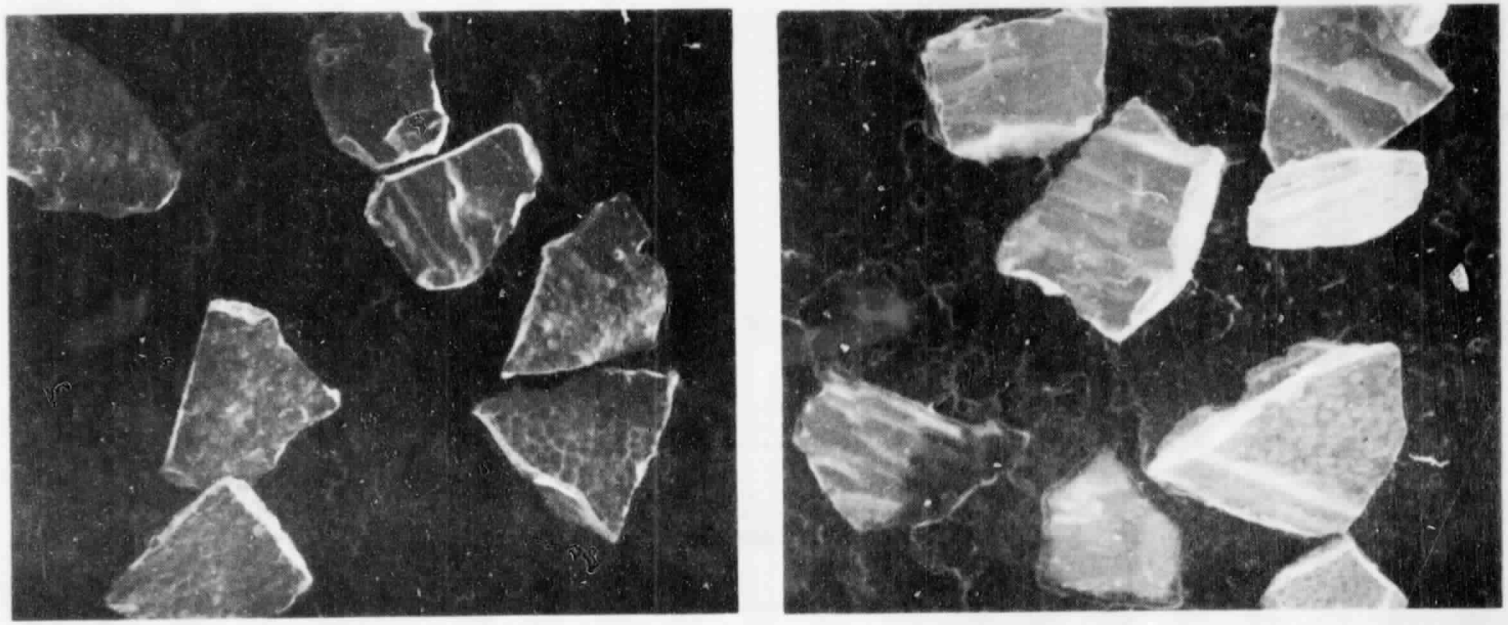

Figure 14. SEM photographs of the prealloyed $NiAl_3$ powder used in the study.

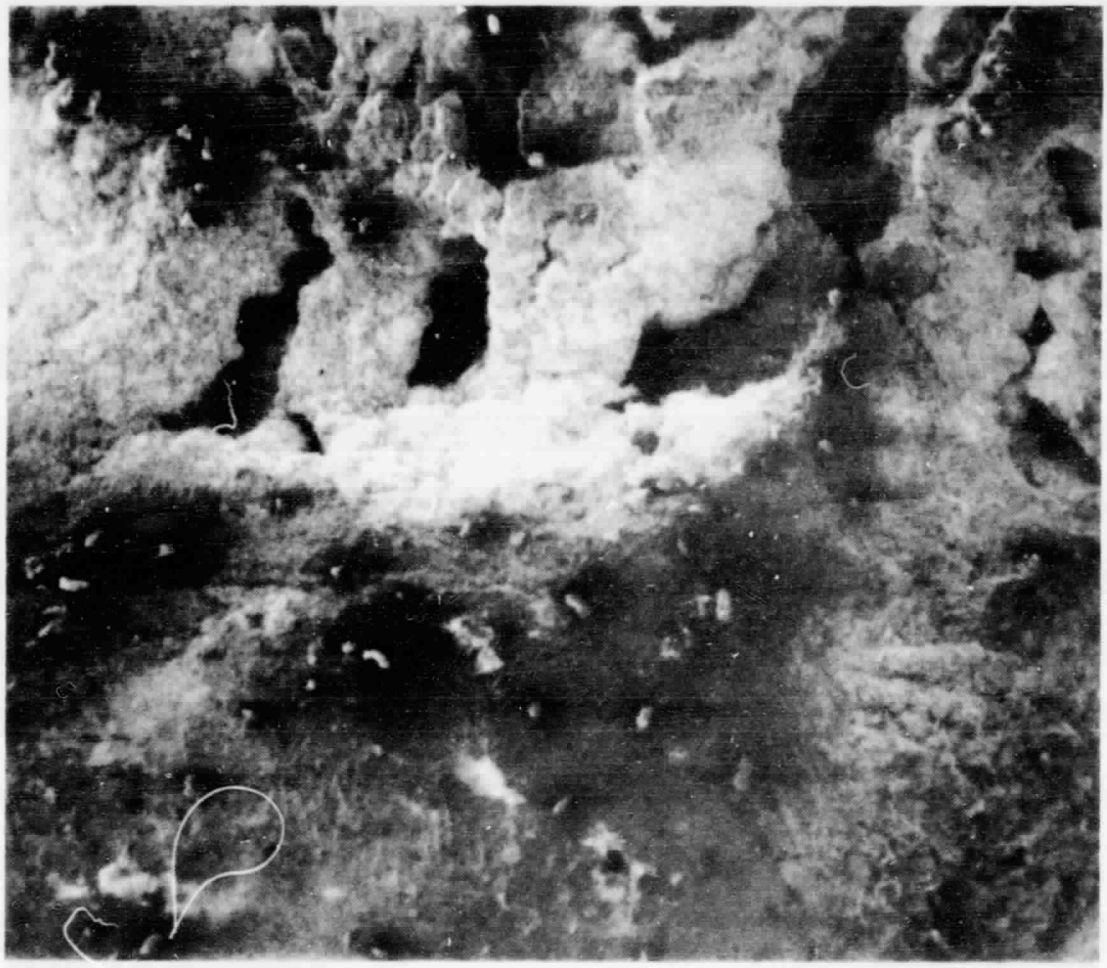

Figure 15. SEM micrograph of an unconsolidated sample that failed to melt and flow out of the crucible orifice.

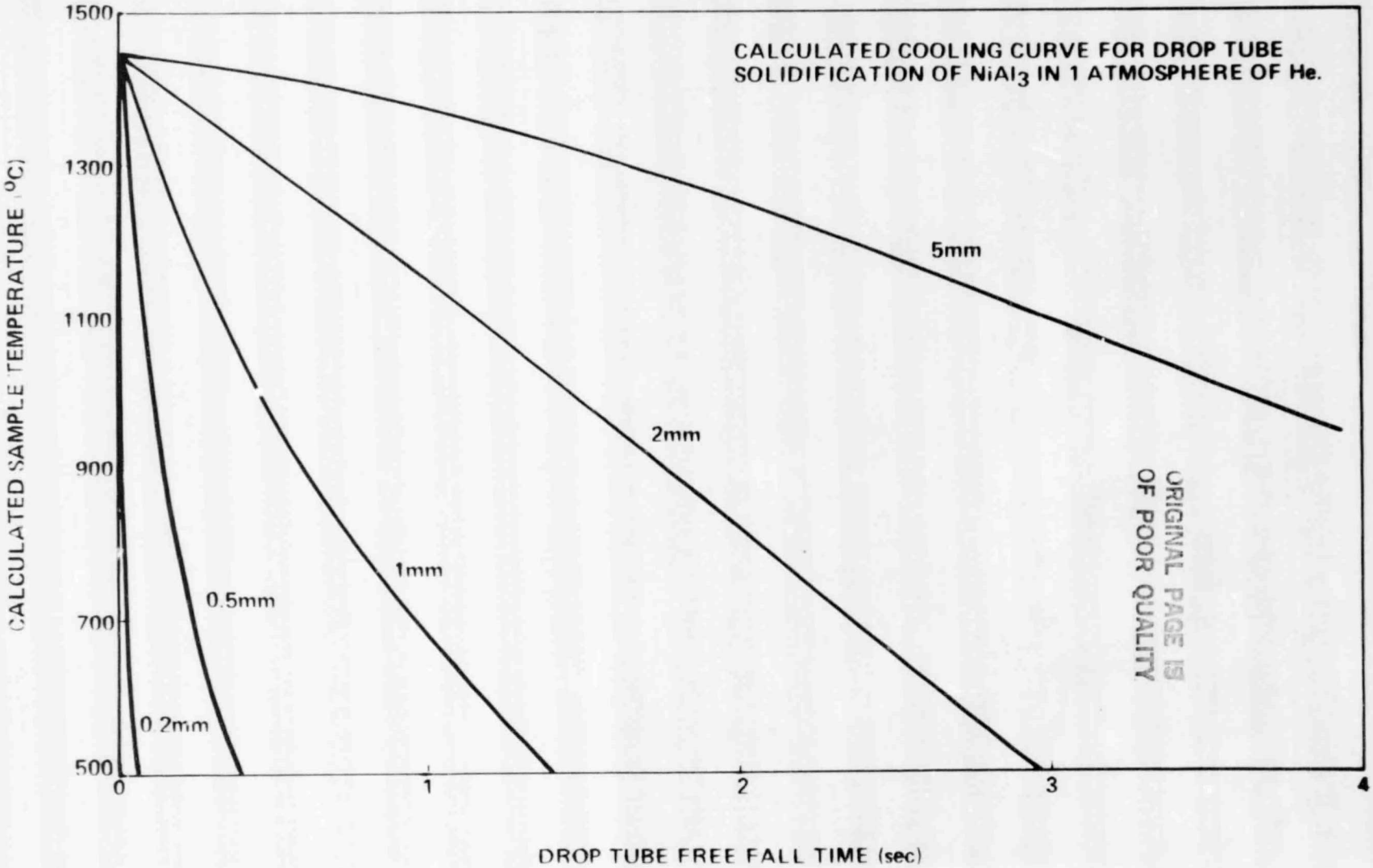

Figure 16. Calculated cooling curves for $NiAl_3$ cooling while falling through 760 torr He gas.

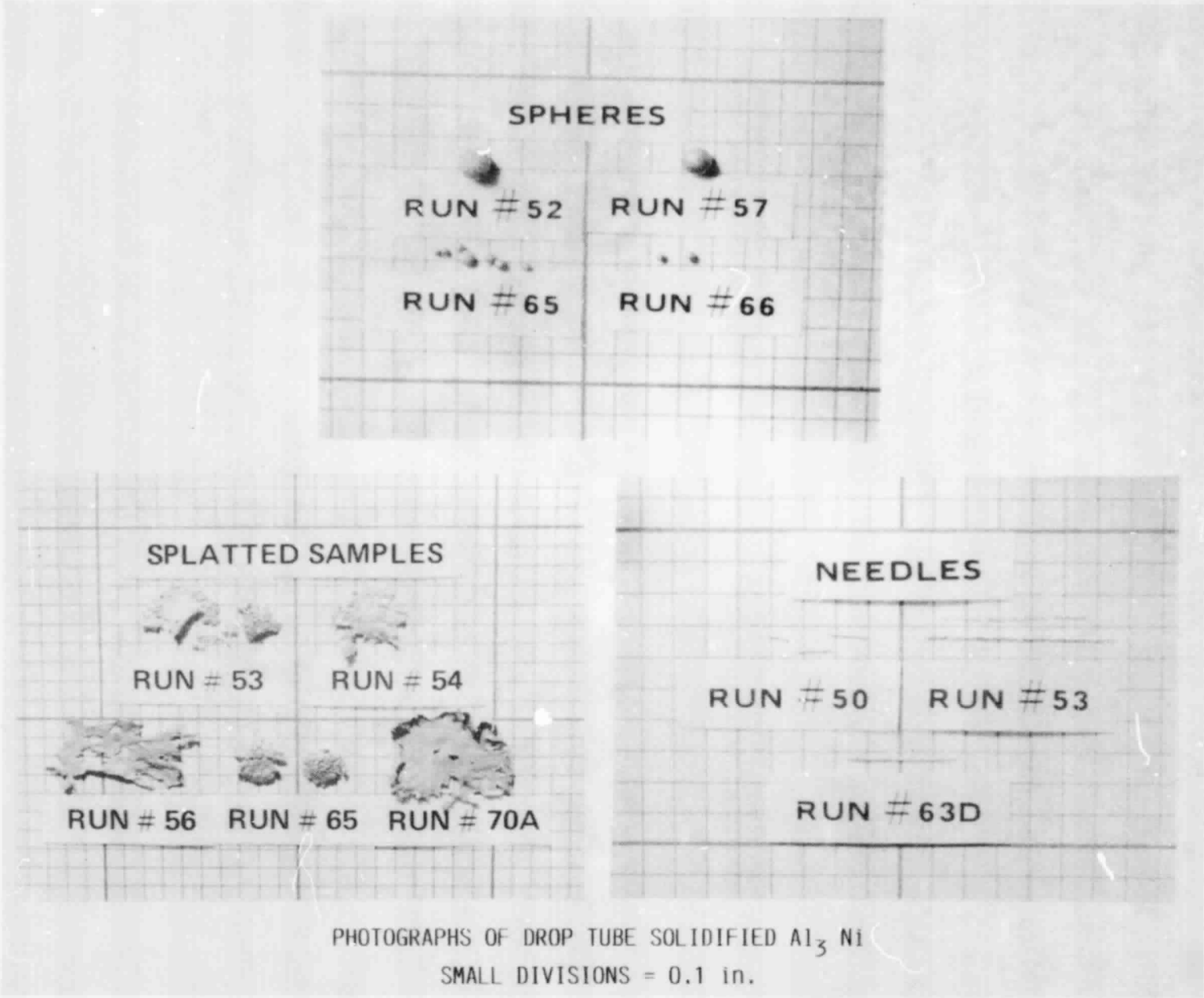

PHOTOGRAPHS OF DROP TUBE SOLIDIFIED $Al_3 Ni$

SMALL DIVISIONS = 0.1 in.

Figure 17. Photographs of drop tube spheres, needles, and splats.

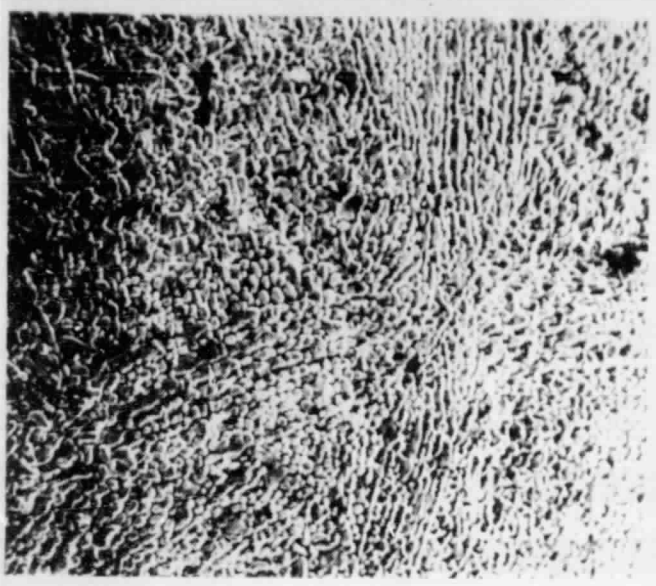

Al_3Ni SPHERE, 0.65mm DIAMETER
DROP TUBE SOLIDIFICATION, 400X

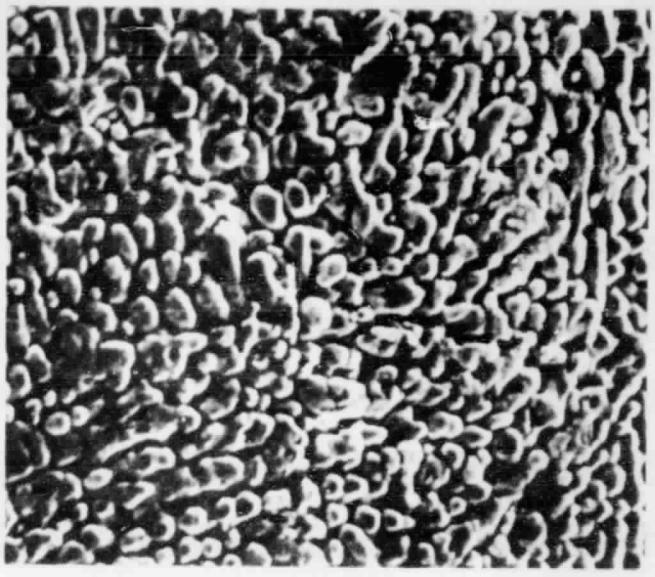

AL_3Ni SPHERE, 0.65mm DIAMETER
DROP TUBE SOLIDIFICATION, 1000X

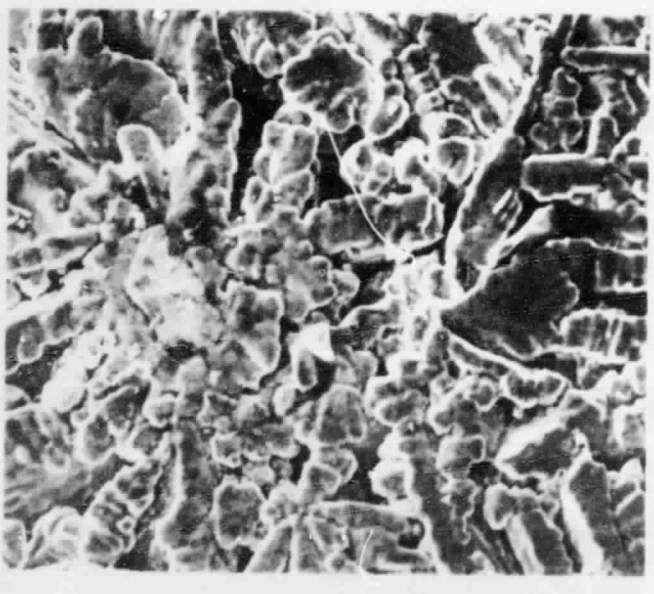

Al_3Ni SPHERE, 1.7mm DIAMETER
DROP TUBE SOLIDIFICATION, 400X

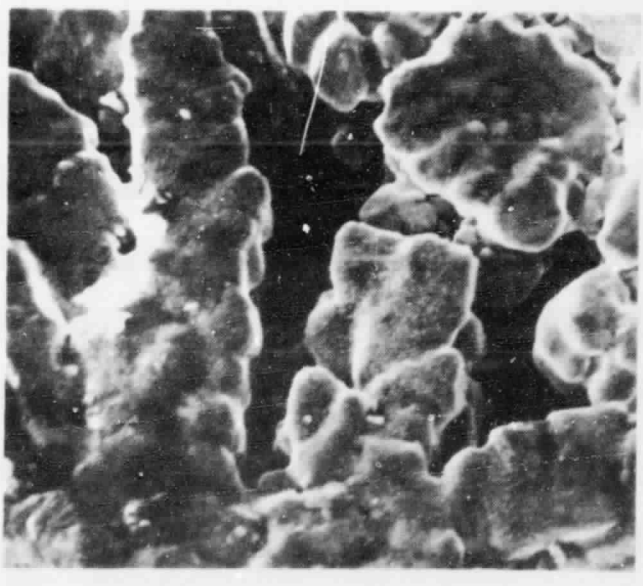

Al_3Ni SPHERE, 1.7mm DIAMETER
DROP TUBE SOLIDIFICATION 1000X

Figure 18. SEM micrographs of the spherical drop tube samples.

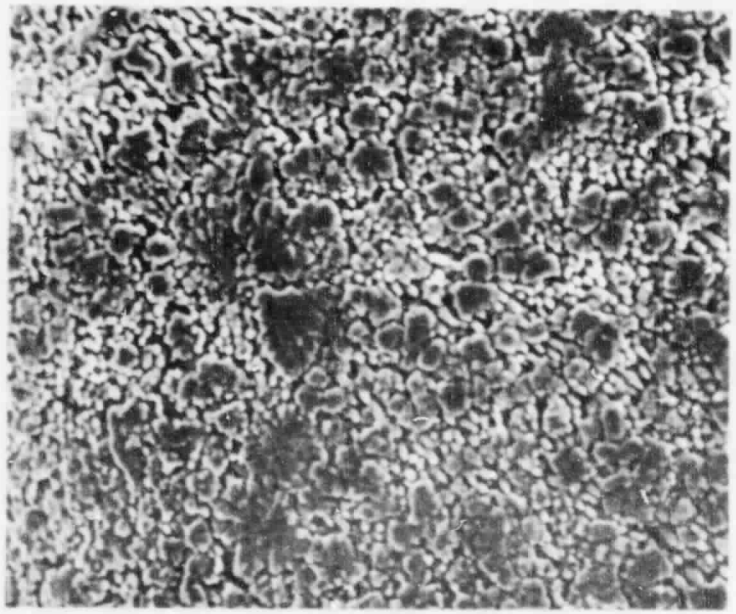

10μm

Al_3Ni NEEDLE, 0.23mm DIAMETER
DROP TUBE SOLiDIFICATION, 1000X

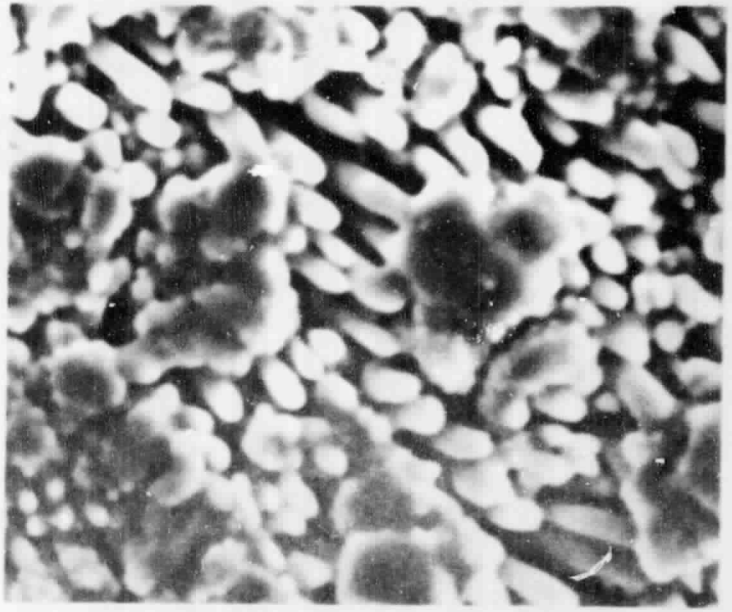

2.5μm

Al_3Ni NEEDLE, 0.23mm DIAMETER
DROP TUBE SOLIDIFICATION, 4000X

Figure 19. SEM micrographs of the drop tube produced needles.

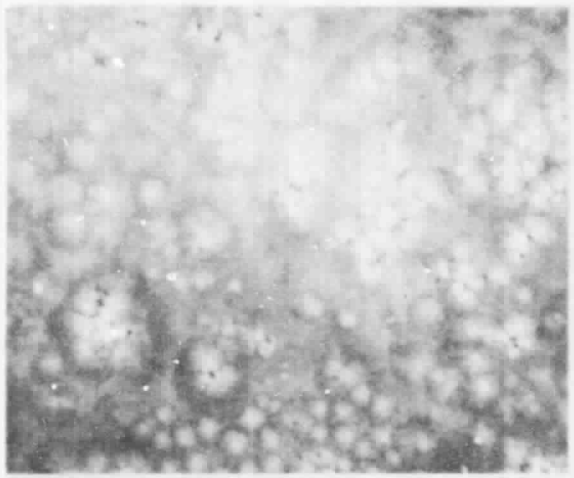

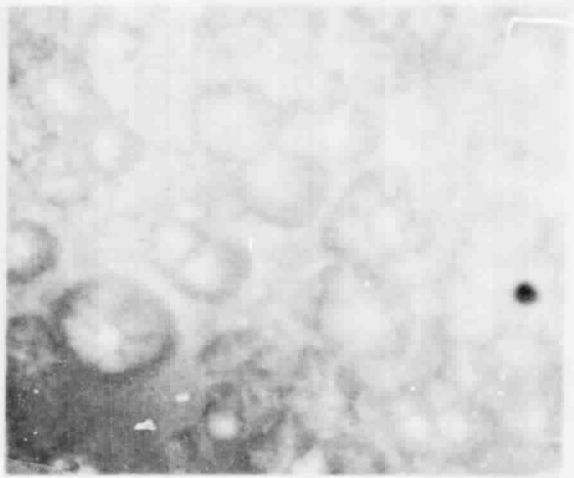

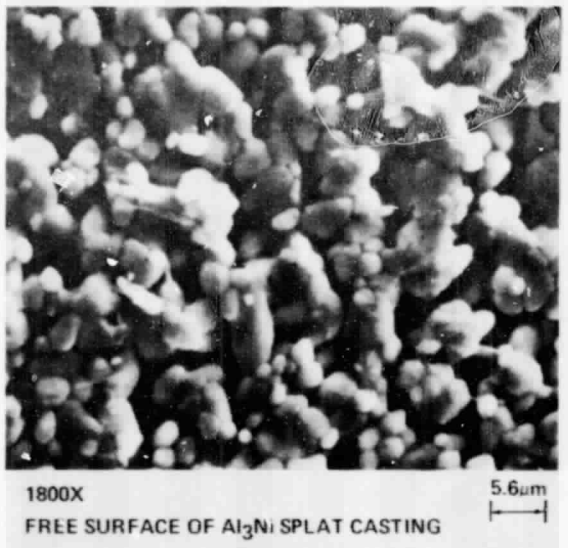

Figure 20. SEM micrographs of splatted samples.

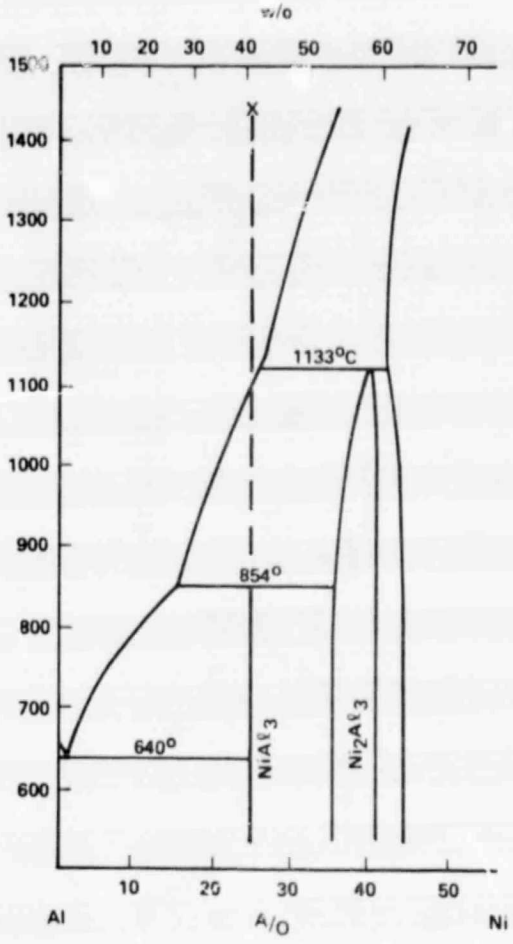

Figure 21. Phase diagram of the Ni-Al system.

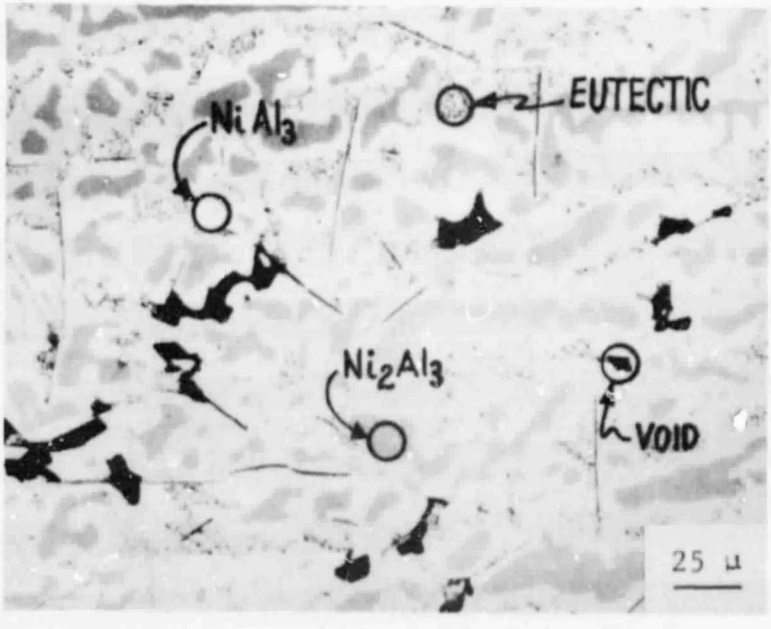

Figure 22. Light micrograph with the phases present in the Ni-Al alloy labeled.

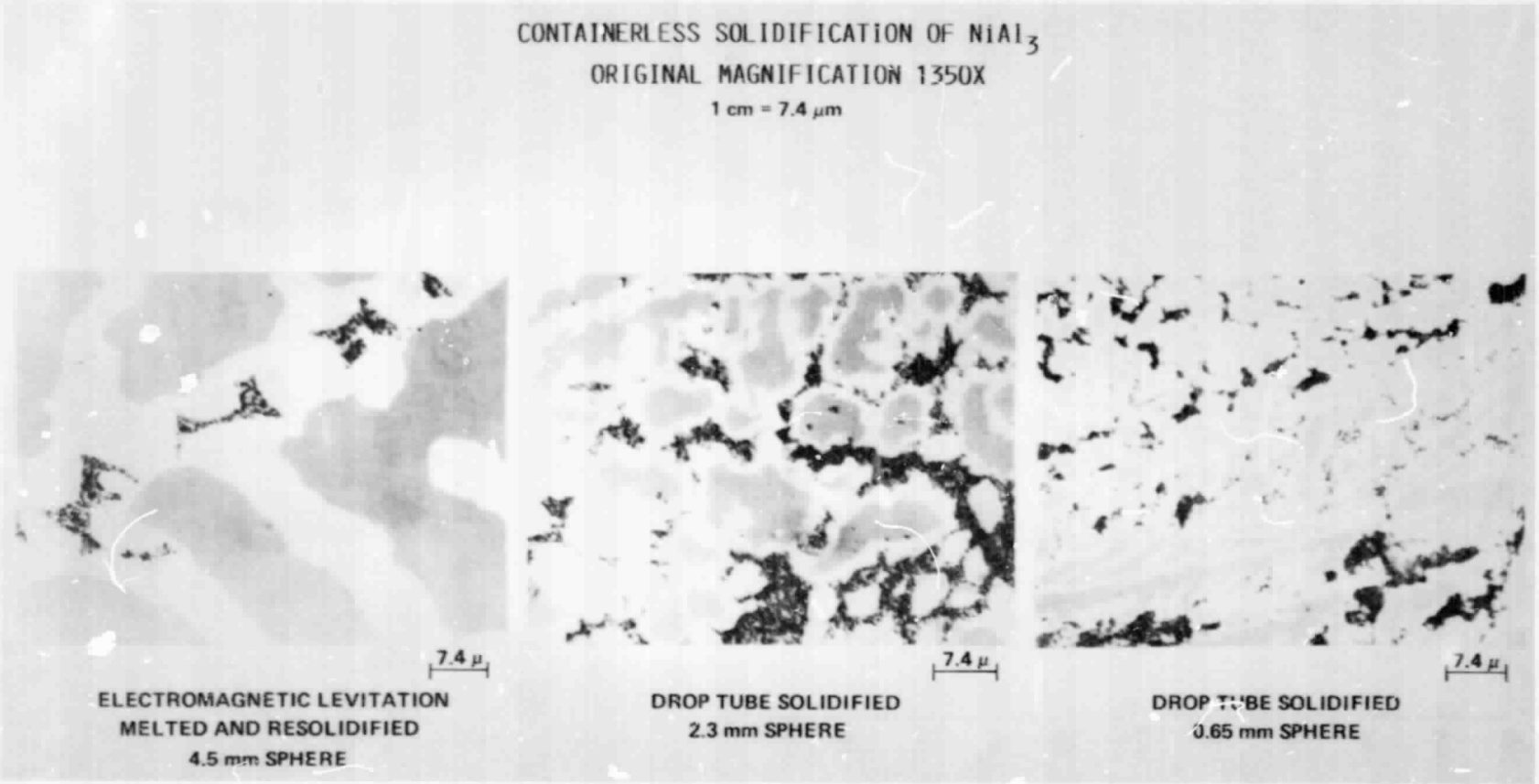

Figure 23. Light micrographs of containerlessly solidified samples.

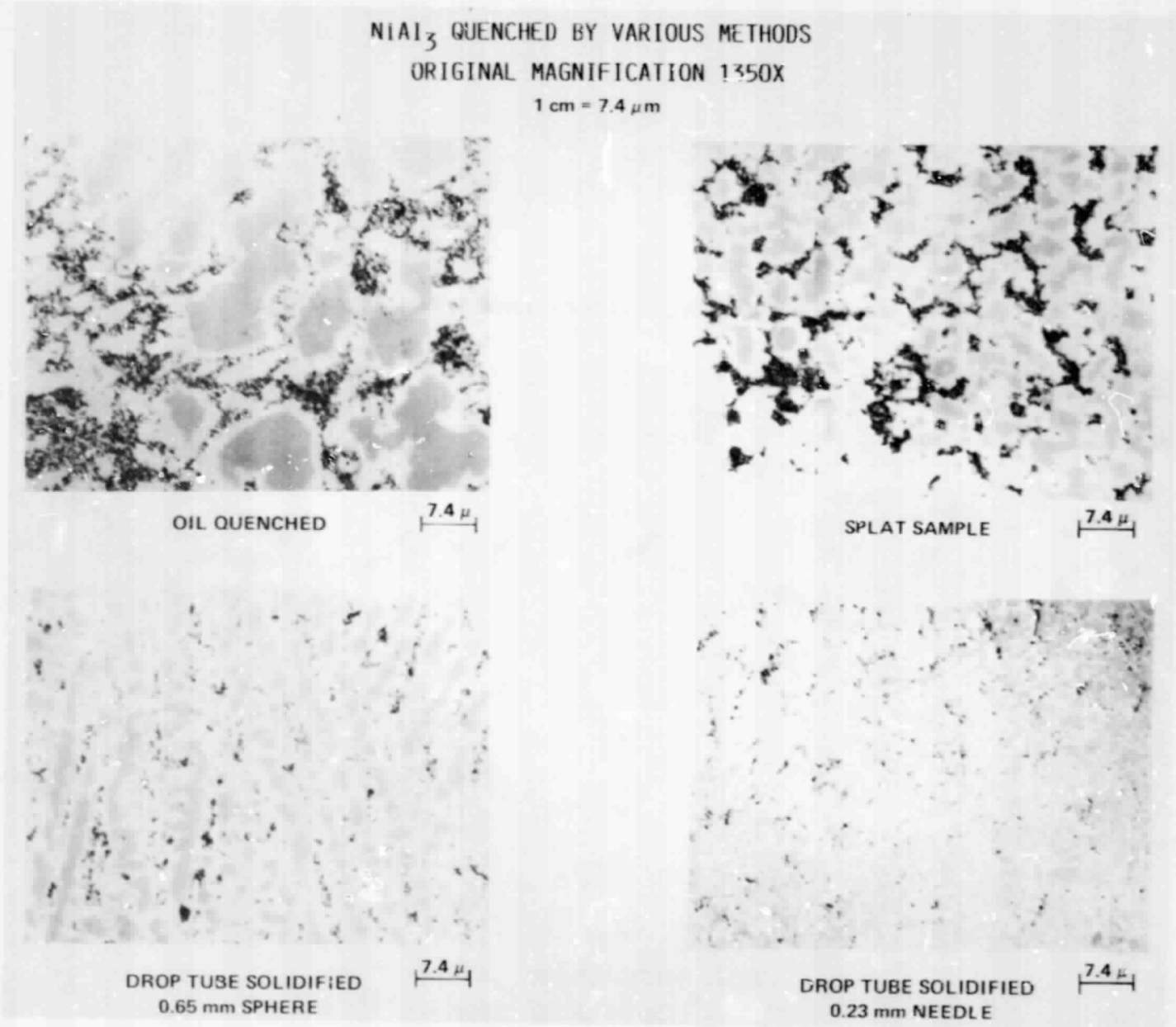

Figure 24. Light micrographs of samples quenched by various techniques.

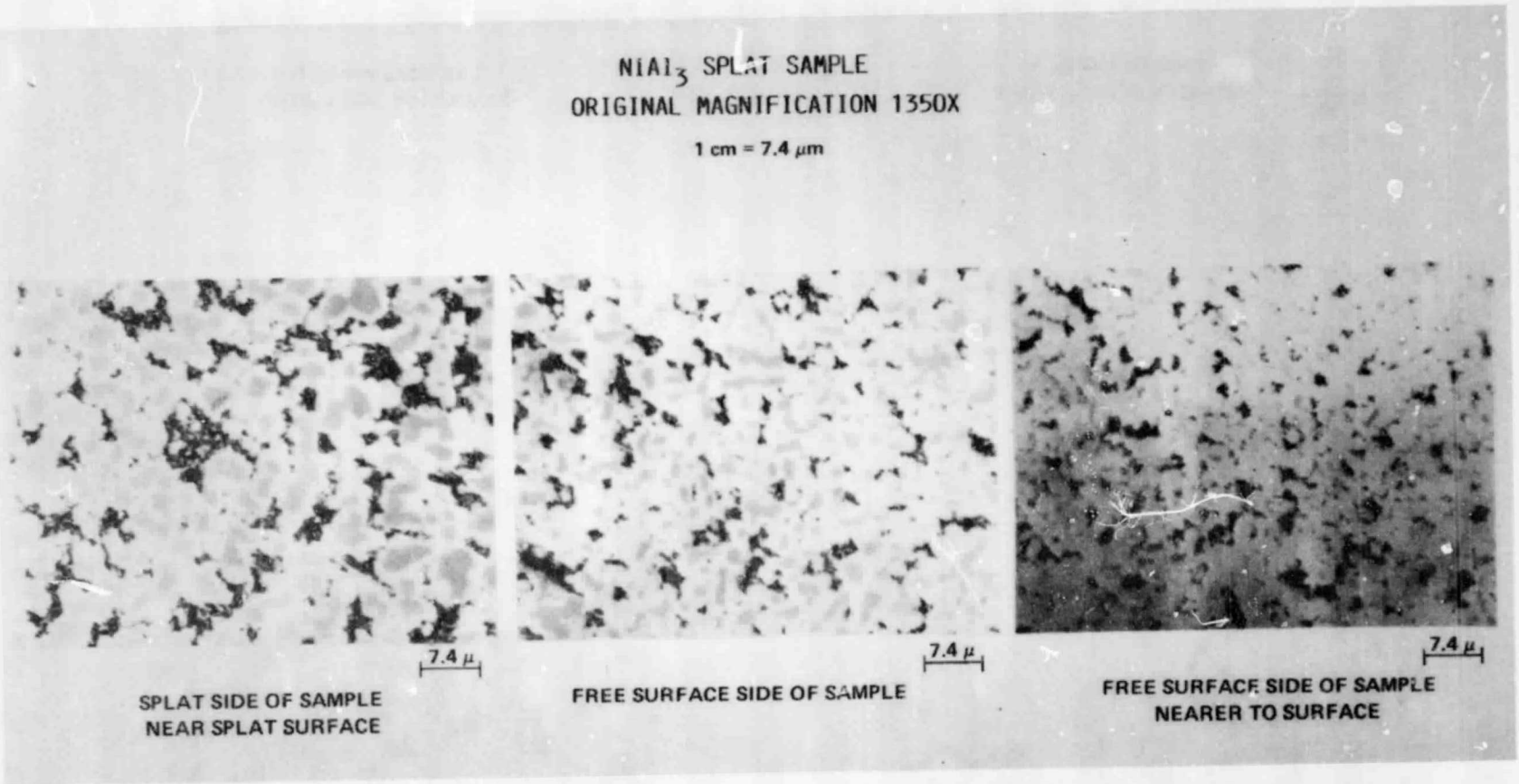

Figure 25. Light micrographs of splatted samples.

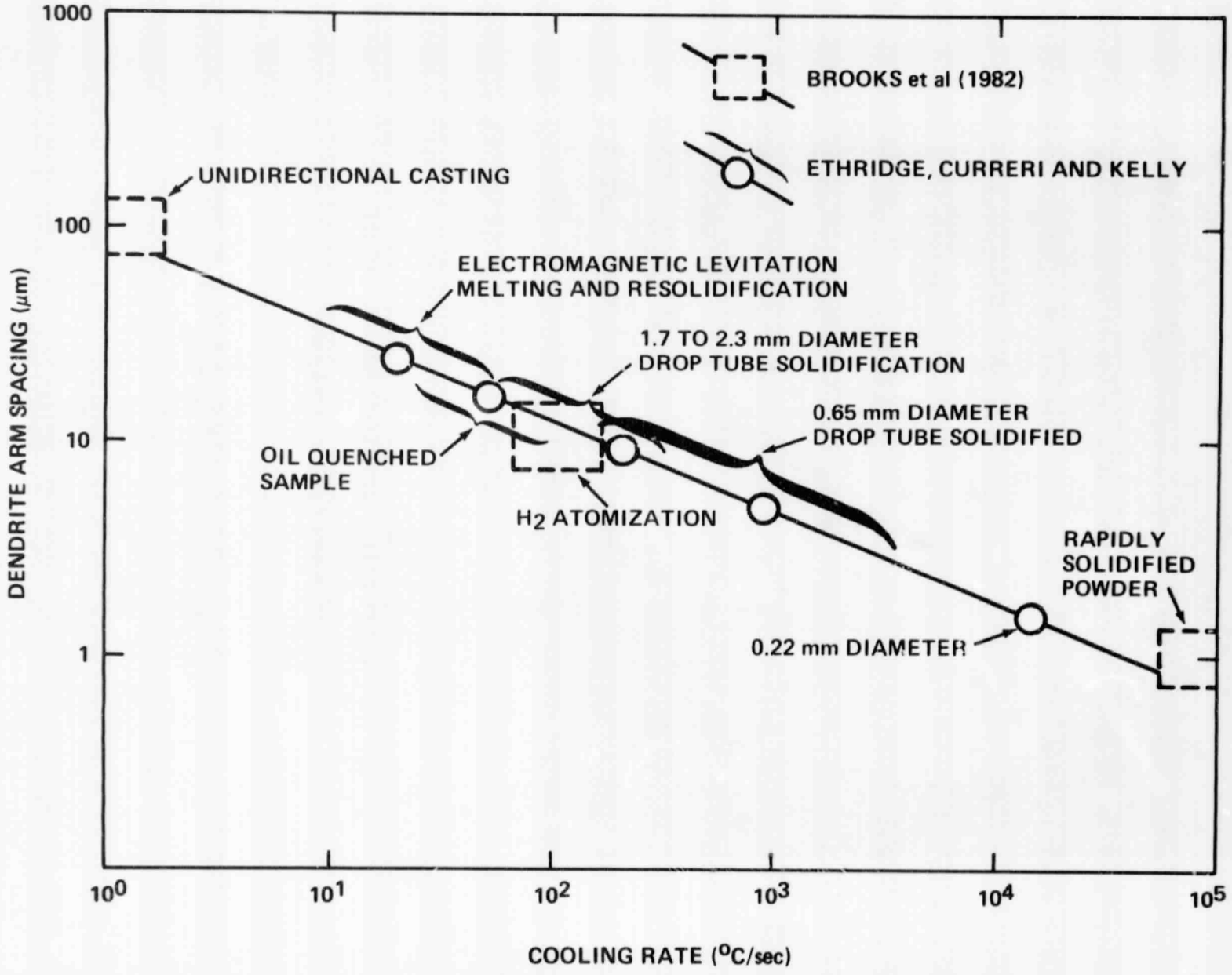

Figure 26. Plot of Dendritic Arm Spacing (DAS) versus cooling rate.

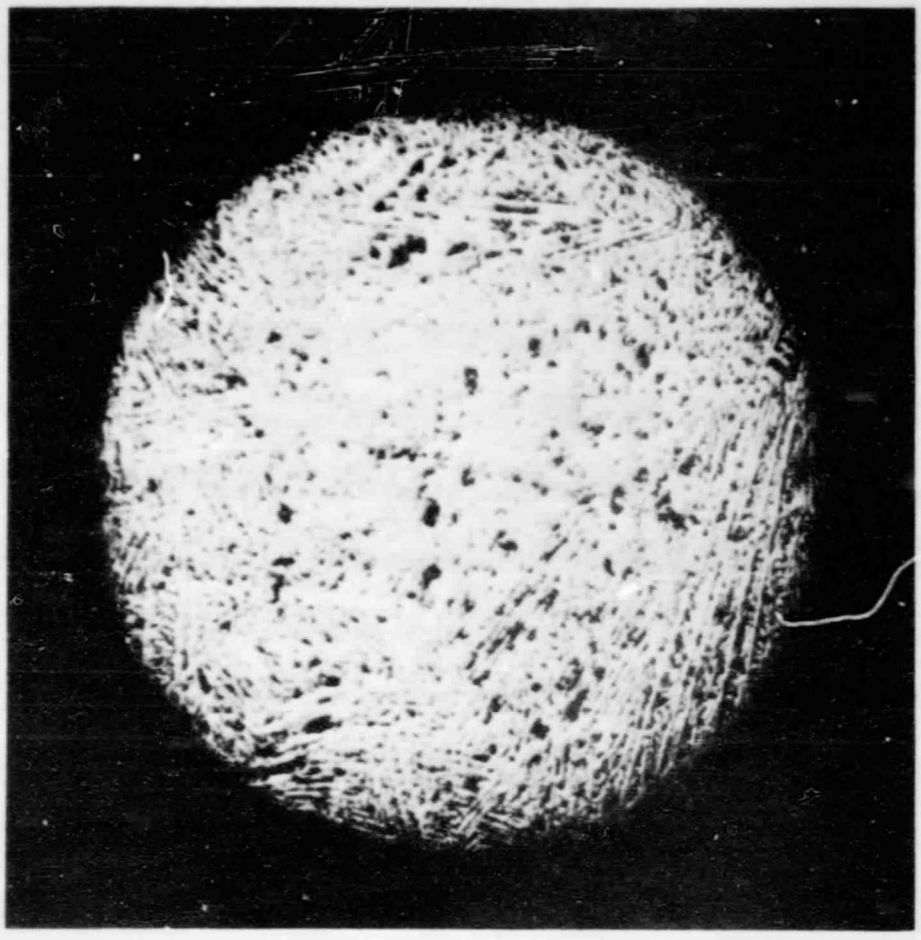

Figure 27. Light micrograph of a sample showing dendrites that originate at the sample surface.

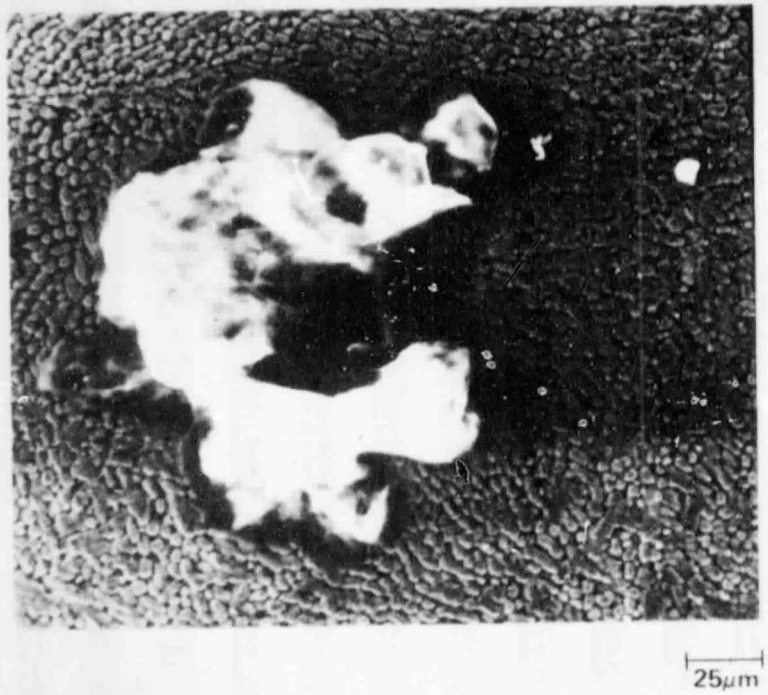

0.65 DIAMETER Al_3Ni DROP TUBE SPHERE WITH INCLUSION, 400X

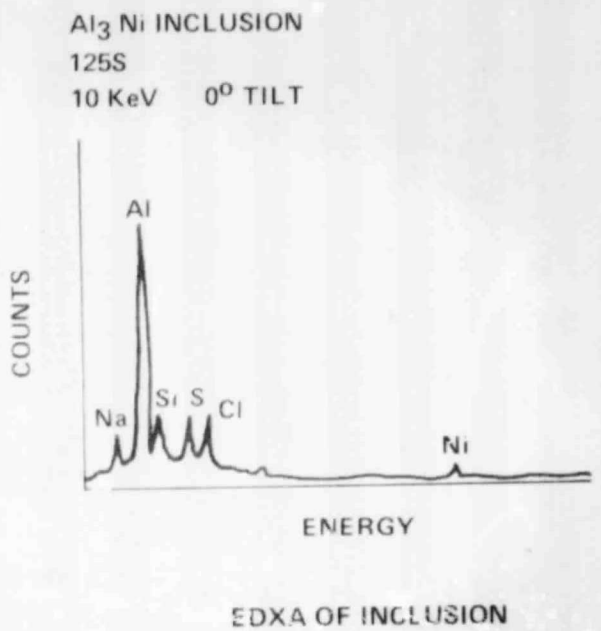

EDXA OF INCLUSION

Figure 28. SEM of the surface of a sphere showing an Al-rich particle.